74TR6

DESIGN AND TEST OF A PUMP FAILURE ANTICIPATOR

By

John L. Frarey
Donald S. Wilson
Richard F. Burchill

Prepared under Contract No. NAS8-30381

SHAKER RESEARCH CORPORATION
Northway 10 Executive Park
Ballston Lake, New York 12019

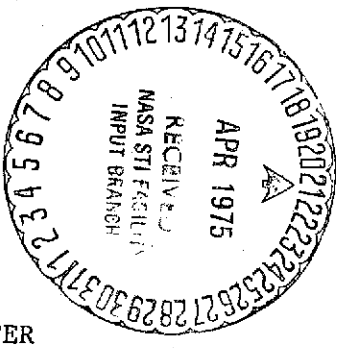

For

NASA-GEORGE C. MARSHALL SPACE FLIGHT CENTER

TABLE OF CONTENTS

LIST OF ILLUSTRATIONS

LIST OF ILLUSTRATIONS
(Continued)

INTRODUCTION

Reliability of mechanical components used in boosters and spacecraft has been the subject of extensive and successful effort by NASA in connection with its wide variety of space programs. Much of this effort centered around careful life tests of units to assure that their design was capable of the minimum life requirements. A new dimension has been added to the effort by the requirement to assess the reliability of components of the space shuttle. In this program, both the shuttle and its booster will be reused. Particularly for the booster, this reuse is planned after what in the past would have been considered a destructive experience of a relatively high g impact followed by salt water emersion. This reusable concept, by definition, means that only those components that would fail during the next planned mission will be replaced. This places NASA in the new business of component refurbishment, checkout, and reuse.

The purpose of this program was to develop a concept and a system that could be used with pumps to allow a rapid judgement to be made of the suitability of the pump for further service. The concept chosen after initial study was the extension of NASA-developed technology based on the processing of high-frequency vibration. This technology is described in References 1 through 3 and more briefly in the second section of this report.

Tests were conducted on two different types of pump (a positive displacement internal gear pump and a shroudless centrifugal pump) in order to refine the concept and to finalize design details on the system to be utilized for pump failure anticipation. Results of this testing are summarized in the body of the report and are supported by detailed data analysis contained in the appendices of this report.

Following the fabrication of the pump failure anticipator, the unit was used for final verification testing with the centrifugal pump. Final circuit modifications that were suggested by the verification testing were included in the unit.

In summary, the program as required by the Request for Proposal provided the classical approach to problem solution:

1. Formulate a concept.
2. Conduct testing to provide design details.
3. Fabricate the diagnostics system.
4. Test the diagnostics system.

The Conclusions and Recommendations portion of this report reviews the degree of success attained by this approach to diagnostic equipment development.

PROPOSED CONCEPT

Following a review of diagnostic concepts that would be applicable to a wide variety of pumps, it was concluded that the high-frequency vibration analysis technique as originally developed under a previous NASA program for the detection of ball bearing defects in a control moment gyro would be the most promising technique for application to the present program. The results of this work were reported under Contract NAS8-25706 in References 1 and 2. The concept as it applies to other mechanical components was discussed in Reference 3. A further review of the literature shows that the above work was predated by work done by Balderson, Reference 4, in which he showed the presence of high-frequency resonances produced by defective ball bearings but did not discuss the demodulation of these signals. Other investigators are utilizing high-frequency vibration in different manners than the proposed concept. Description of these variations on the proposed method are contained in References 5 and 6. A comprehensive review of many different vibration techniques used for diagnostic purposes is included in Reference 7.

The proposed concept is based on the fact that when a mechanical component is impacted, it will ring at one of its natural or resonant frequencies--normally the lowest mode. When lower modes are restrained by mounting clearances, higher unrestrained modes will resonate. In general, the high modes are not restrained due to the fact that the extremely small deflections associated with even high g levels are many times smaller than the surface finish of the mating surfaces.

In addition to high-frequency resonances being excited by impacts, they can be excited by rolling or sliding contact between two surfaces in somewhat the manner of the familiar chalk squeal on a blackboard. Again, low-frequency resonances can be damped out by the fit up tolerances of parts while high-frequency resonances can still be free to ring.

In an assembly of mechanical components such as a pump, some impacts and rubs will normally occur even for a well-operating pump. As the pump condition deteriorates, the impacts and rubs generally become more severe. Different types of pumps, however, can produce quite different g levels of high-frequency resonances for normal operation. The two pumps tested during this program are excellent examples of this variation. Figure 1 shows two high-frequency spectra. Figure 1a comes from a normally-operating, shroudless centrifugal pump with very low level impacts and rubs. Figure 1b comes from an internal gear pump in distress. Even a normally-operating gear pump shows much higher impacts or rubs than one encounters in the centrifugal pump.

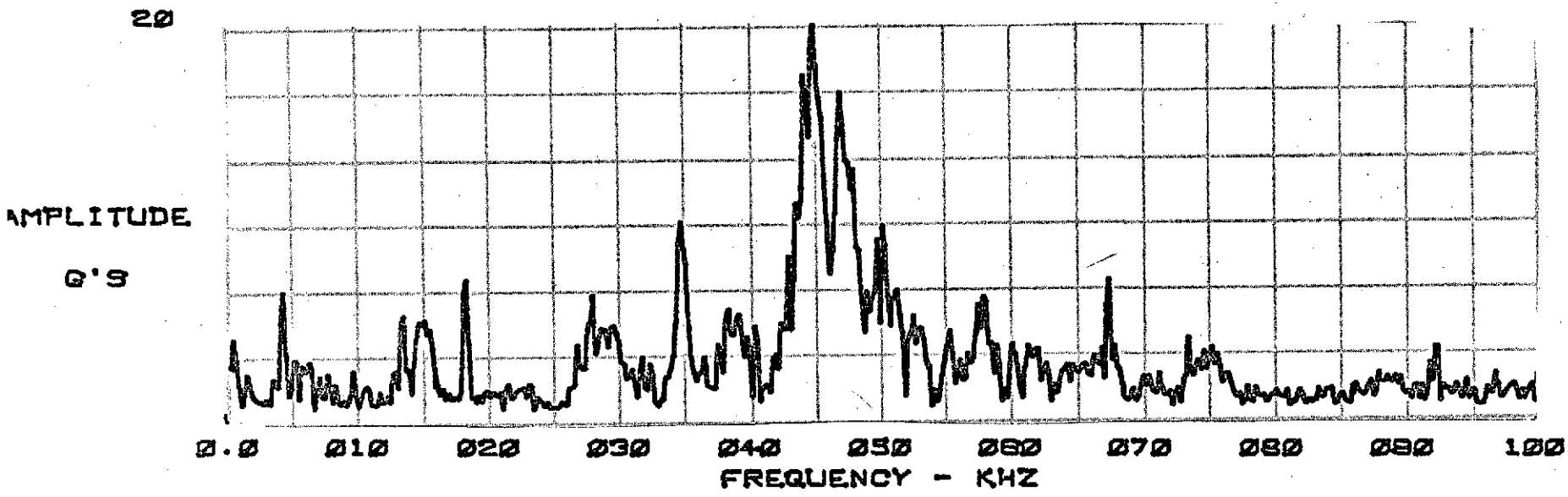

B GEAR PUMP

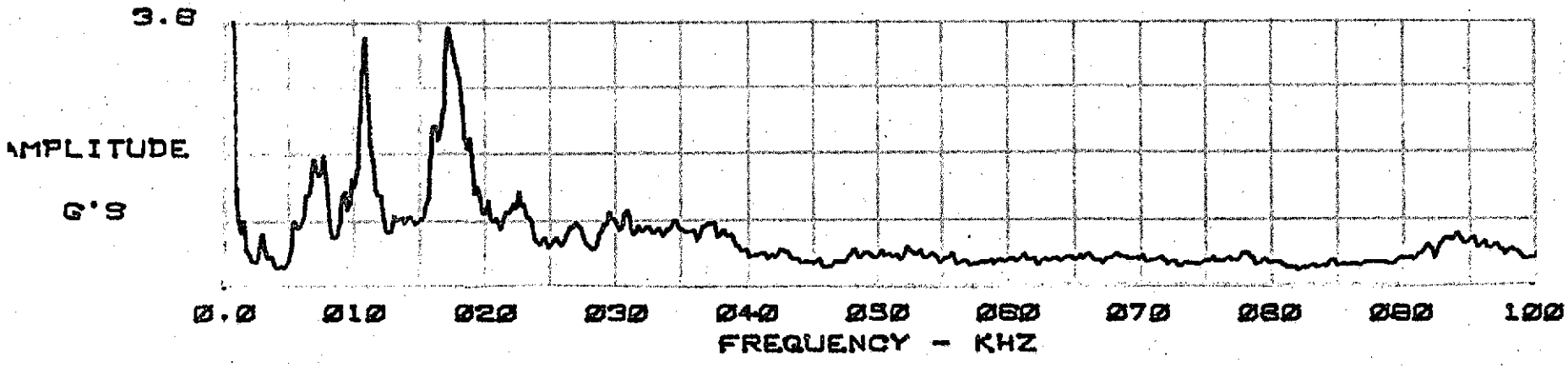

A CENTRIFUGAL PUMP

FIGURE 1 HIGH FREQUENCY SPECTRA, CENTRIFUGAL AND GEAR PUMP

A diagnostic concept could be proposed that simply uses the g level in the high-frequency spectrum as the indicator of component conditions. It will be shown that, particularly for the internal gear pump, this can be a valid criteria for overall condition. The use of this criteria alone, however, can be insufficient to adequately warn of some types of impending failures; and, as proposed, should be amended to allow the better understanding of the nature of the source of the excitation of the high-frequency resonances.

Additional information could be gained if each resonance were identified as to which portion of the pump is ringing. The process of this identification would be very tedious and would still not directly relate in all cases to the source of the excitation. This is because some components such as the pump casing can be excited by more than one diagnostically important event.

A better way to determine the source of the resonance excitation is to filter the resonance out from all other signals and examine its amplitude versus time characteristics. Figure 2 is the appearance of such a signal taken by filtering the 28 KHz resonance produced by the centrifugal pump. The regular impact and decay of the resonance may be observed. The timing between impacts relates to the rotational rate of the ball about its own axis in the ball bearing of the drive motor for the pump. Figure 3 is another amplitude versus time trace of a filtered resonance--this one taken from the internal gear pump. It is clear that more than one type of event is taking place with the timing of the two events apparently harmonically related. In this case, the repetition rates and amplitudes of the impacts are due to the interaction of the gear mesh impact and the rotation of the gear itself. It quickly becomes apparent that trying to identify the source of the resonance excitation by observing the oscilloscope picture of the filtered resonance can get quite complicated and certainly does not lend itself to an efficient system for quick component checkout.

Several techniques can be used to treat the data if the high-frequency (carrier frequency) could be illuminated and only the upper envelope of the signal retained. If this is done, the repetition rate of a high-frequency signal is converted to a low-frequency signal. The process that accomplishes this signal transformation is called envelope detection or demodulation. It is the same process used in A.M. radios to recover the audio signals from the high-frequency carrier. In Figure 4, the bottom trace is the time varying high-frequency resonance. The top trace is the envelope of the high-frequency resonance that is obtained by demodulating the signal of the lower trace.

Once the signal has been transferred from the high-frequency region to the low-frequency region, filters can be used to determine the frequency of repetition and, therefore, locate the source of the impact or rub that excites the high-frequency resonance. A convenient instrument

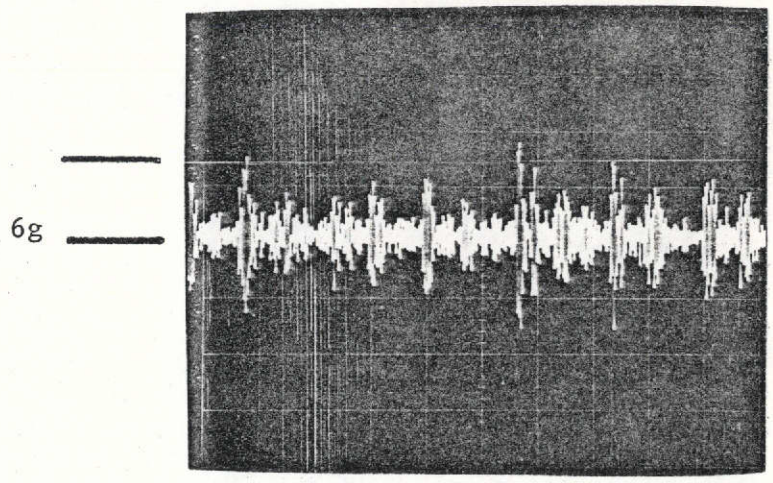

FIGURE 2 AMPLITUDE VS. TIME TRACE (28KHz) OF DEFECTIVE BEARING - CENTRIFUGAL PUMP

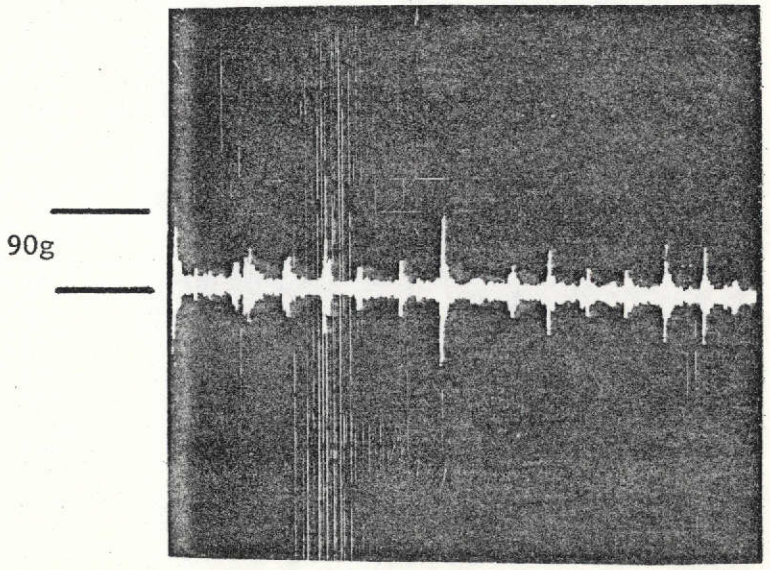

FIGURE 3 AMPLITUDE VS. TIME TRACE (45KHz) OF INTERNAL GEAR PUMP - SIMULATED WEAR

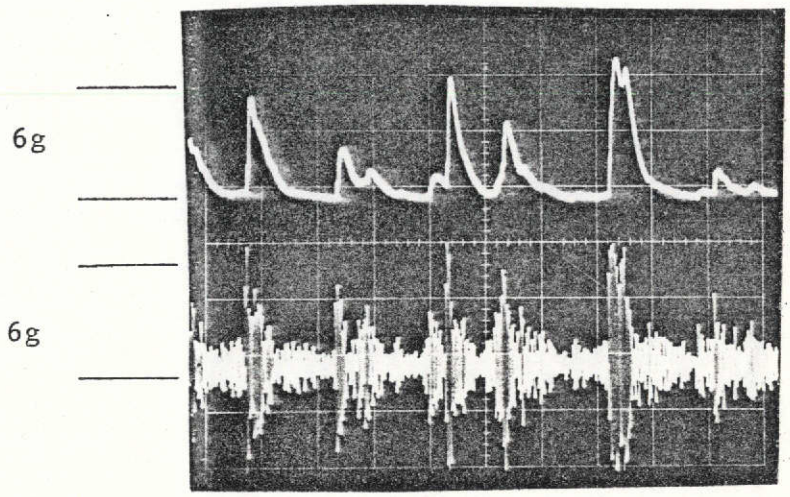

FIGURE 4 TOP - ENVELOPE DETECTED RESONANCE

BOTTOM - AMPLITUDE VS. TIME TRACE (28KHz RESONANCE) OF DEFECTIVE BEARING--SAME AS FIGURE 2

to display the frequency content of the envelope data for report and laboratory purposes is the real time spectrum analyzer. This device allows the plotting of the amplitude versus frequency of the envelope. Figure 5 is the spectra of the envelope shown in Figure 4. The pump failure anticipator that is described later in this report is based on the vibration envelope detector principal.

A note of caution is required in assigning amplitudes to the signals discussed above, whether it be the amplitude of the resonance or the frequency content of the envelope. Comparing the amplitude versus time trace of Figure 4 with the spectra of the envelope (Figure 5), there appears to be a discrepancy. This may be explained by noting that the amplitude scale for Figure 4 is peak g's for the composite signal while the amplitude of the envelope spectra is peak g's for a given frequency component of the composite signal. Likewise, the g levels assigned to the overall resonance amplitude taken from a spectra such as in Figure 1 will be the equivalent amplitude of a signal at that frequency that remains constant over the memory time of the real time analyzer rather than the transient type of signal shown in Figure 2. In this report, g levels reported will always be accompanied by a statement as to how they were measured.

The following steps summarize the concept chosen for test and evaluation in this program:

1. High-frequency resonances are identified and their amplitudes measured.
2. The high-frequency resonance is band pass filtered and demodulated.
3. The frequency content of demodulated signal is determined.
4. From the frequency of excitation and a knowledge of the pump mechanism, the source of the excitation can be determined.
5. The amplitude of the signal at the given frequency is determined.
6. Decisions on the condition of the pump are made based on the amplitude of the resonance, the frequency content of the envelope, and the amplitude of the frequency components of the envelope.

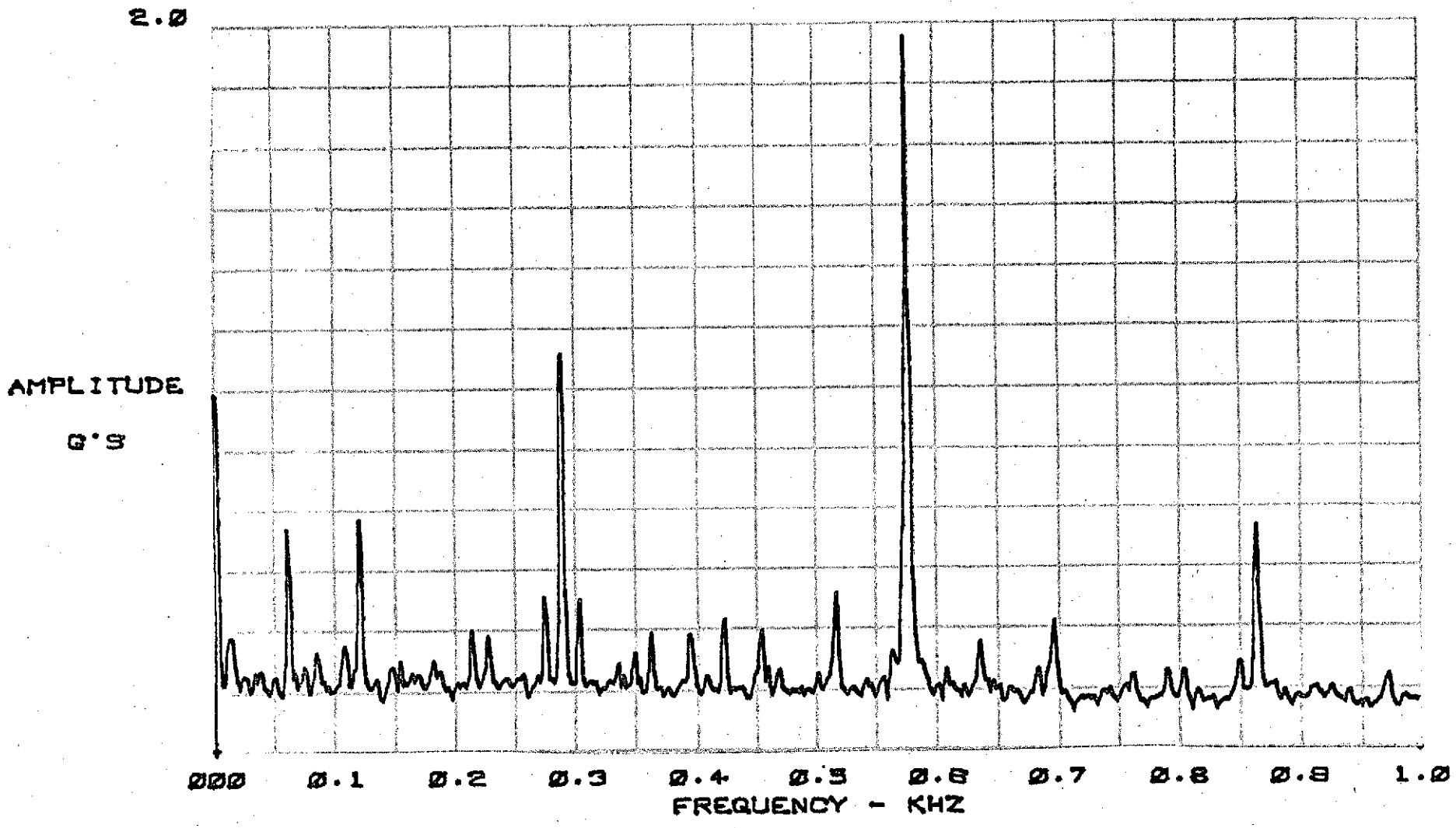

FIGURE 5 DEMODULATED SPECTRUM OF DEFECTIVE BEARING - CENTRIFUGAL PUMP. SIGNALS AT 286 AND 572 ARE BALL DEFECT SIGNALS.

PUMP AND FLOW BENCH DESCRIPTIONS

The pump originally selected for this program was a commercial grade internal gear pump. This pump was selected because it allowed the study of different failure modes. NASA suggested that the final testing of the failure detection system include a pump more representative of flight hardware even though these pumps are designed to have a much more limited number of probable failure modes. NASA agreed to furnish the pump used to pump the coolant for the Skylab ATM. This is a dual, unshrouded centrifugal pump manufactured by AiResearch.

Internal Gear Pump

The 3 gpm, 100 psid test pump configuration is illustrated schematically in Figure 6. A photo of the disassembled pump is shown in Figure 7. The smaller internal gear or idler is supported and rotates on a hardened pin. The outer gear is the driven member and is supported by two bushings with a face seal between the two bushings. The outer sleeve is a porous bronze oil-impregnated bushing that is exposed to ambient environment by virtue of the seal. The inner bushing is a carbon bushing lubricated by the pumping media.

The configuration is a typical type internal gear pump with the internal gear driven by the outer and separated in the lower half of the bore by the seal crescent. This type pump was selected since a number of wear areas exist providing an ideal vehicle to demonstrate the usefulness of high-frequency vibration to detect not only the wear but the component in distress. The primary areas where wear might be anticipated include:

a. Gear tooth wear

b. Internal gear bore and support pin wear

c. Crescent wear from internal gear outer diameter and external gear inner diameter

d. Carbon bushing wear

e. Porous bushing wear

During operation of the pump, as discharge pressure is increased at the pump discharge, the pressure loads the inner gear downward toward the crescent and the outer gear upward against the crescent. Wear in any of the bushings or inner gear support journal will cause contact of the gears against the crescent.

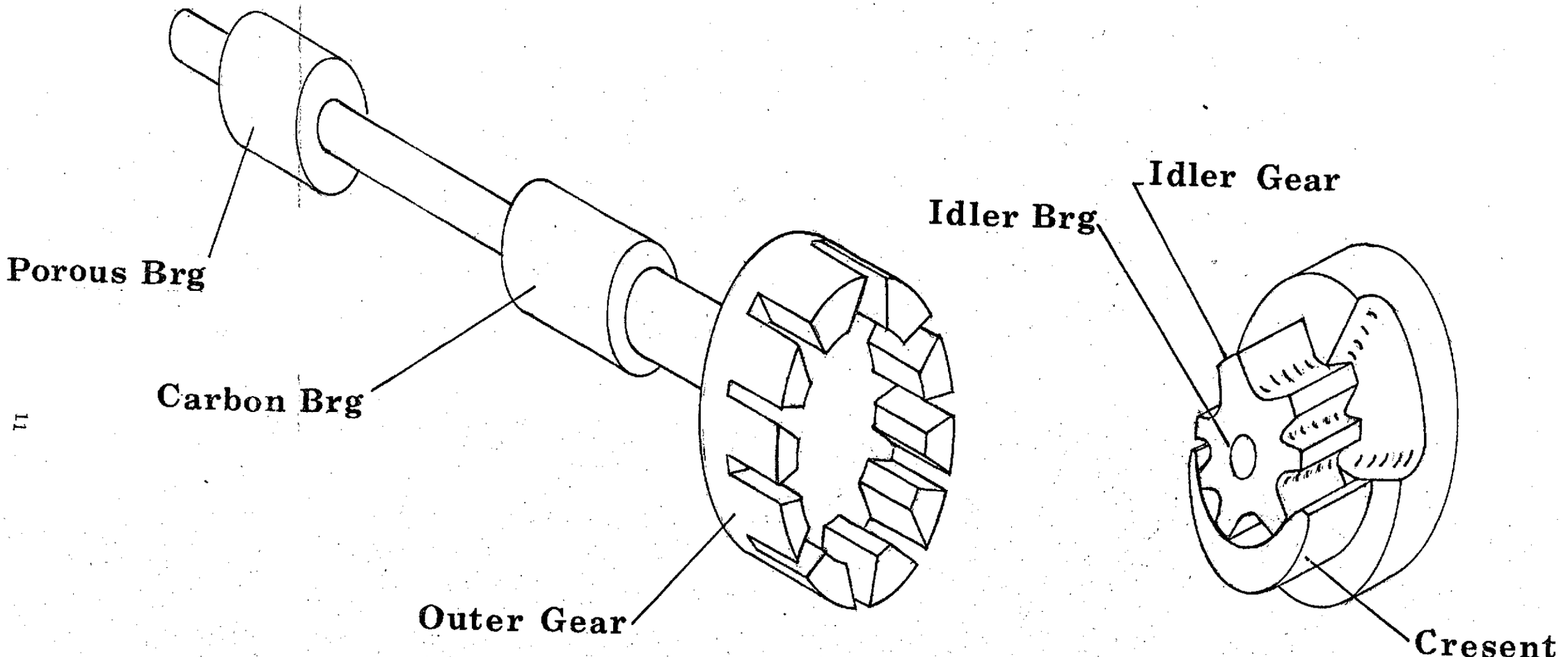

FIGURE 6 SCHEMATIC OF INTERNAL GEAR PUMP

FOLDOUT FRAME

FOLDOUT FRAME

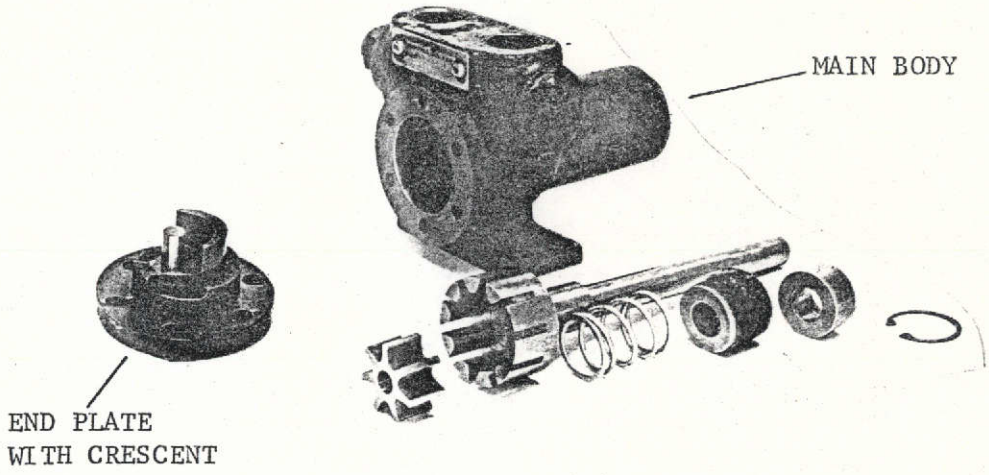

FIGURE 7a

VIKING MODEL FH32-D PUMP

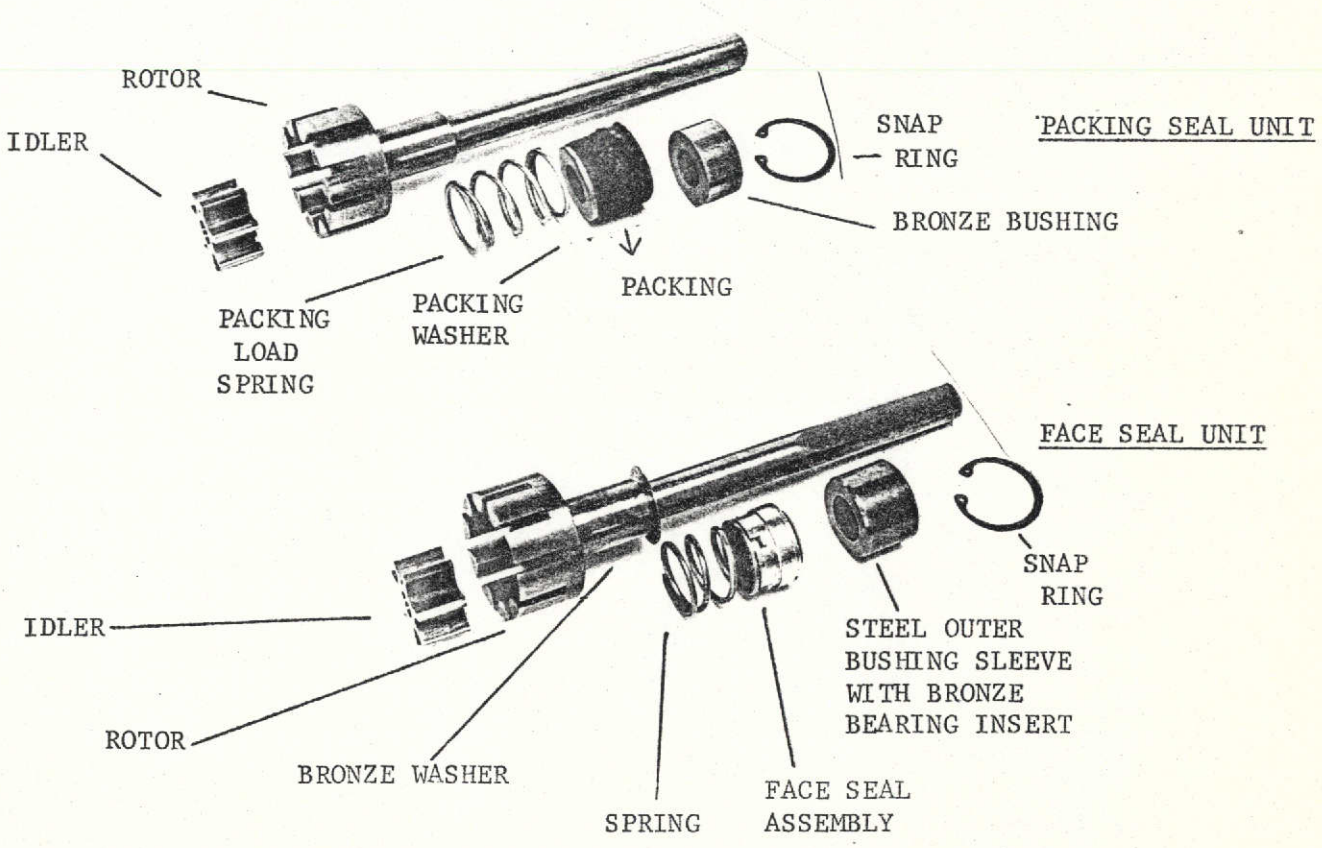

FIGURE 7b

PUMP INTERNAL COMPONENTS

One additional point of interest in reviewing the data is a constructional feature of the pump. The idler gear, its support journal pin, and the seal-crescent form an assembly which pilots in the pump body. Because the pilot diameter fit is approximately .002 inches loose in the housing, it is possible during pump assembly to shift the idler-crescent subassembly relative to the outer gear. Internal pump clearances are such that the crescent can be moved into contact with the outer gear inner diameter. As discharge pressure from the pump is increased, the outer gear is further loaded against the crescent. When assembled properly, the outer gear does not contact the crescent even under loading. However, when the assembly insures adequate outer gear to crescent clearance, it changes the gear mesh pitch line contact condition between idler and outer gears. The use of this pump, therefore, allows the concept to be evaluated not only for wear failures but also for incorrect assembly following teardown and inspection.

Centrifugal Pump

The AiResearch pump used for evaluation of the failure anticipator is depicted in Figure 8. The pump incorporates the dual-motor, dual-pump redundant concept, each unit of which is capable of delivering 900 lbs/hr of water at a pressure rise of 31 psi (minimum).

The pump impeller is an open centrifugal impeller with six cantilevered straight blades. The impeller diameter is 1.39 inches. The fluid is discharged through a single conical diffuser. The design is inherently insensitive to face clearance, impeller-shroud contour match and particle ingestion.

The four-pole, three-phase motors have a 99.75 percent aluminum rotor cage for improved speed-torque characteristics.

The magnetic coupling was sized to transmit 6.0 in-oz of torque minimum. It consists of two concentric permanent rings, each containing six matching poles.

The pump rotor shaft was designed to be carried by a single journal bearing made of Fibrite material E2748-10275, post-cured (a fiberglass reinforced epoxy with a 10 percent Teflon dispersion). The journal is lubricated by water fluid which fills the entire pump cavity. The bearing, rotor shaft, impeller, and driven magnet are illustrated in Figure 9.

In terms of failure modes, the three-phase motor design can operate on two phases in the event an open is encountered in one phase. This will induce magnetic unbalance in the rotating flux field inducing rotor vibration.

The magnetic coupling has a higher rating than the drive motor and, therefore, slippage of the coupling is not an anticipated failure mode.

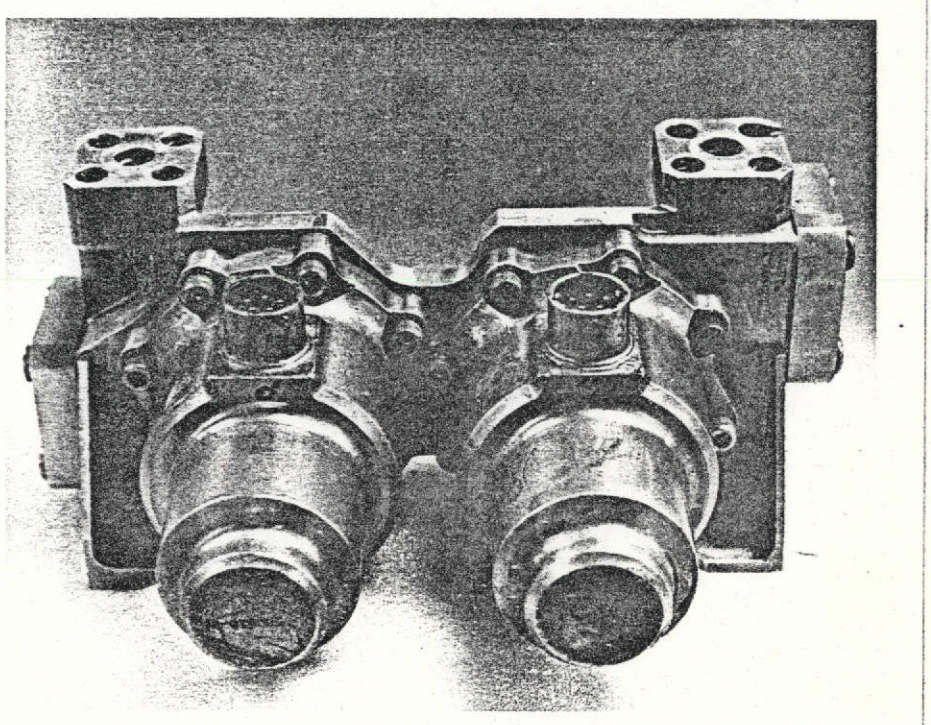

FIGURE 8 DUAL CENTRIFUGAL PUMP

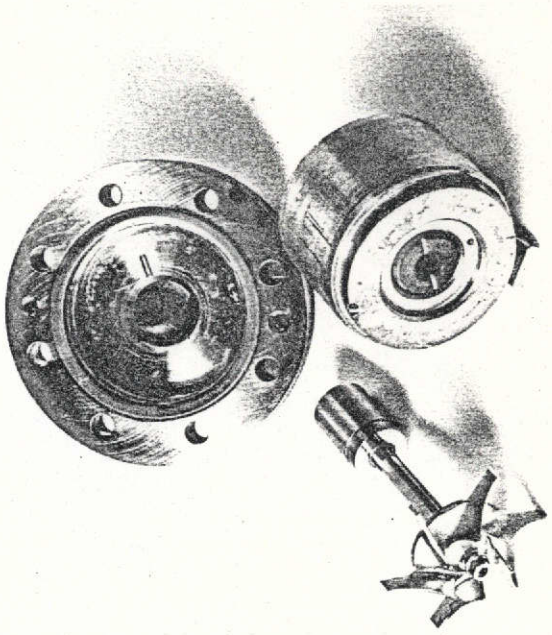

9a PUMP

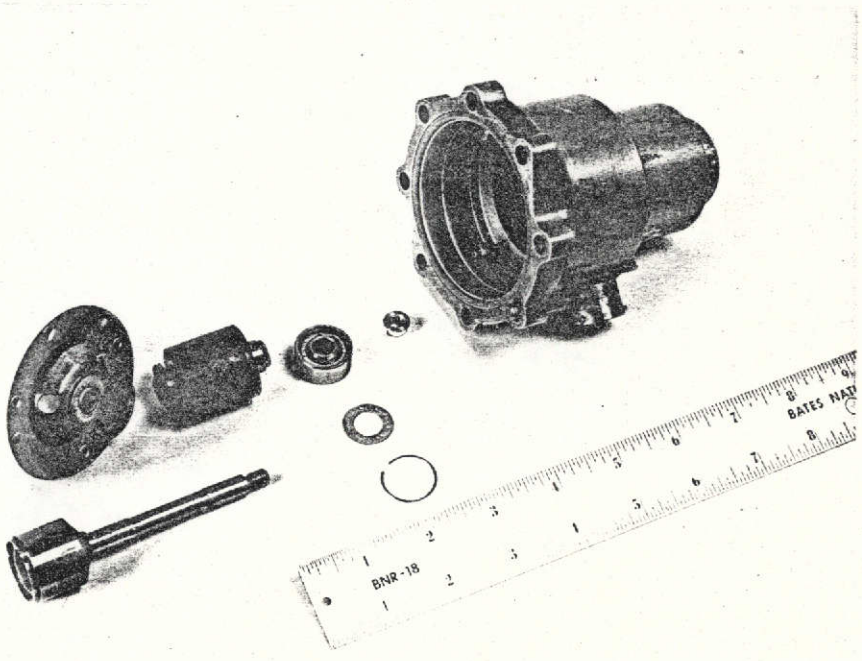

9b MOTOR

FIGURE 9 CENTRIFUGAL PUMP

Rubbing of the magnet on the seal would necessitate a bearing failure which should be detected prior to the rub. Therefore, no failure modes of the coupling were considered.

Relative to the motor, the bearings represent the most vulnerable failure mode. Most classifications of rolling-element failures emphasize the fatigue failure mode. This, in a sense, is unfortunate since small, lightly-loaded, grease-packed bearings fail from lubrication exhaustion. As the lubricant is depleted sufficiently, the separating lubricant film will break down and the rolling elements will come into metal-to-metal contact. The broadband vibration noise will be readily transmitted to the housing structure for ultimate detection prior to failure. Other types of bearing distress such as shock-induced brinelling will result in an intermittent film rupture condition with similar results.

The pump assembly differs from the motor in the support system since hydrodynamic water bearings are used to support the rotating assembly. This type bearing depends on development of a hydrodynamic pressure to lift the rotor and provide separation between the rotating and stationary members. As long as separation is maintained, there is no wear and life is limited only by fatigue induced by dynamic load. Under light load operation this approaches an infinite life. As loads increase and contact occurs, the life becomes a function of the wear rates of the materials in contact. Therefore, detection of those areas where degradation induces higher bearing loads is quite important and would be important to detect. This encompasses increased rotating unbalance loads from impeller erosion, loose impeller or damaged impeller, and increased magnetic loads due to flux unbalance or magnetic eccentricity in the coupling. As in the case of rolling-element bearings where rupture of the elastohydrodynamic film is an important indication of life, detection of rupture of the hydrodynamic film is important in the pump. Changes in the vibration signature due to those areas that can induce rupture as well as detecting the onset of rupture become most important and would be detected.

In addition to the journal bearing, the thrust support in the pump is also hydrodynamic. Therefore, detection of film rupture in the thrust system is equally important. Since thrust loads are a function of the hydrostatic balance in the impeller and back plate regions, vibration analysis over the discharge pressure range with a trend of increasing high-frequency amplitudes with pressure would be indicative of thrust system distress.

Test Facility

A pump test facility was designed and fabricated to allow testing of both pumps. The setup is shown schematically in Figure 10. Figure 11 is a photograph of the system in use with the internal gear pump. The facility allowed testing each pump from no flow to its maximum flow

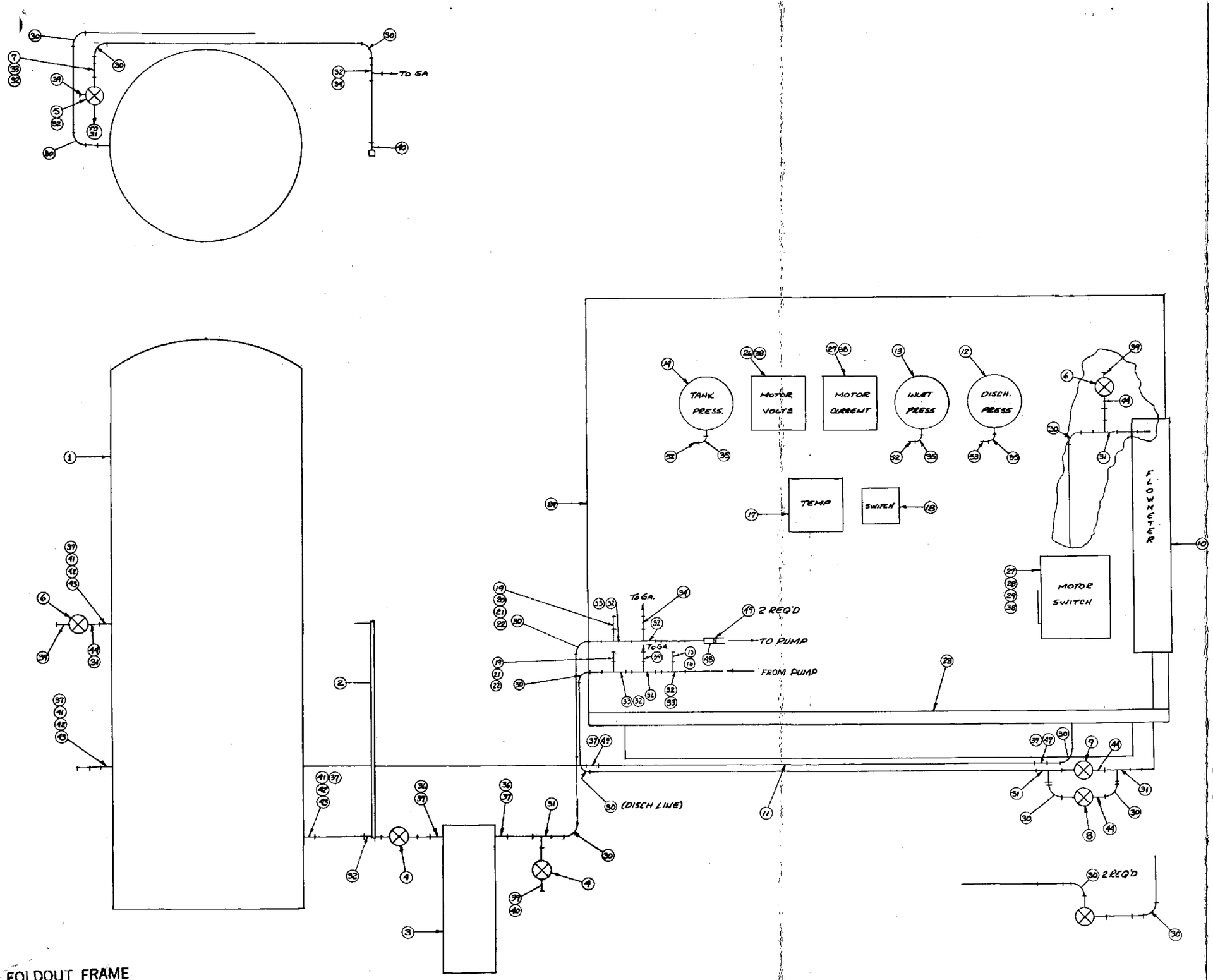

FOLDOUT FRAME

FIGURE 10 FOLDOUT FRAME 2

ORIGINAL PAGE IS
OF POOR QUALITY

DIMENSIONAL TOLERANCES UNLESS OTHERWISE SPECIFIED FRACTIONS ± 1/32	SHAKER RESEARCH CORPORATION NORTHWAY 10 EXECUTIVE PARK BALLSTON LAKE, NEW YORK 12019		
DRAWN W.D. WALDRON	TITLE PIPING LAYOUT - PUMP FAILURE ANTICIPATOR TEST RIG		
SCALE 1"=4"	DRAWING NUMBER SK-D-1025		
EO 31-79	SHEET 1 OF 4	REV	

RST ORDER

PRESENT ORDER

SHAKER RESEARCH CORPORATION
Northway 10 Executive Park
Ballston Lake, N.Y. 12019

NO.

TITLE: PUMP FAILURE ANTICIPATOR TEST RIG - PARTS LIST

REF: SK-D-1025 - Figure 10

QUANTITY G4	G3	G2	G1	ITEM NO.	PART NO.	DESCRIPTION	MATERIAL
				1		Water Tank	
				2		Water Gauge	
				3		Filter	
				4		Gate Valve	
				5		Relief Valve	
				6		Globe Valve	
				7		Air Tank Valve	
				8		Pressure Relief Valve	
				9		Globe Valve	
				10		Flowrater	
				11		Cooling Fins	
				12		Pressure Gage (Pump Discharge)	
				13		Pressure Gage (Pump Inlet)	
				14		Pressure Gage (Tank)	
				15		Pressure Transducer	
				16		Adapter	
				17		Pyrometer	
				18		Thermocouple Switch	
				19		Thermocouple	
				20		Thermocouple (Spare)	

			REVISIONS	DATE	CODE IDENT. NO.	
PREP'D					NO.	
CH'KED						
APPR.						
ISSUED					SHEET NO. 2 of 4	REV.

FIRST ORDER	SHAKER RESEARCH CORPORATION Northway 10 Executive Park Ballston Lake, N.Y. 12019	NO.
PRESENT ORDER		

TITLE: PUMP FAILURE ANTICIPATOR TEST RIG - PARTS LIST

REF: SK-D-1025 - Figure 10

QUANTITY				ITEM			
G4	G3	G2	G1	NO.	PART NO.	DESCRIPTION	MATERIAL
				21		Ferrules (Spare)	
				22		Thermocouple Wire	
				23		Bench	
				24		Plywood	
				25		Voltmeter	
				26		Ammeter	
				27		Motor Switch	
				28		Box Clamp	
				29		Romex	
				30		Elbow	
				31		Tee	
				32		Tee	
				33		Reducing Bushing	
				34		Male Connector	
				35		Female Connector	
				36		Adapter	
				37		Reducing Bushing	
				38		Wire	
				39		Hose Coupling	
				40		Adapter	

			REVISIONS	DATE	CODE IDENT. NO.	
PREP'D					NO.	
CH'KED						
APPR.						
ISSUED					SHEET NO. 3 of 4	REV

RST ORDER

PRESENT ORDER

SHAKER RESEARCH CORPORATION
Northway 10 Executive Park
Ballston Lake, N.Y. 12019

NO.

TITLE: PUMP FAILURE ANTICIPATOR TEST RIG - PARTS LIST

REF: SK-D-1025 - Figure 10

QUANTITY G4	G3	G2	G1	ITEM NO.	PART NO.	DESCRIPTION	MATERIAL
				41		Reducing Bushing	
				42		Male Adapter	
				43		Reducing Bushing	
				44		Adapter	
				45		Reducer	
				46		Elbow	
				47		Coupling	
				48		Hose	
				49		Hose Clamp	
				50		Pipe	
				51		Pipe Strap	
				52		Tubing	
				53		Tubing	
				54		Coupling	

			REVISIONS	DATE	CODE IDENT. NO.	
PREP'D					NO.	
CH'KED						
APPR.						
ISSUED					SHEET NO. 4 of 4	REV.

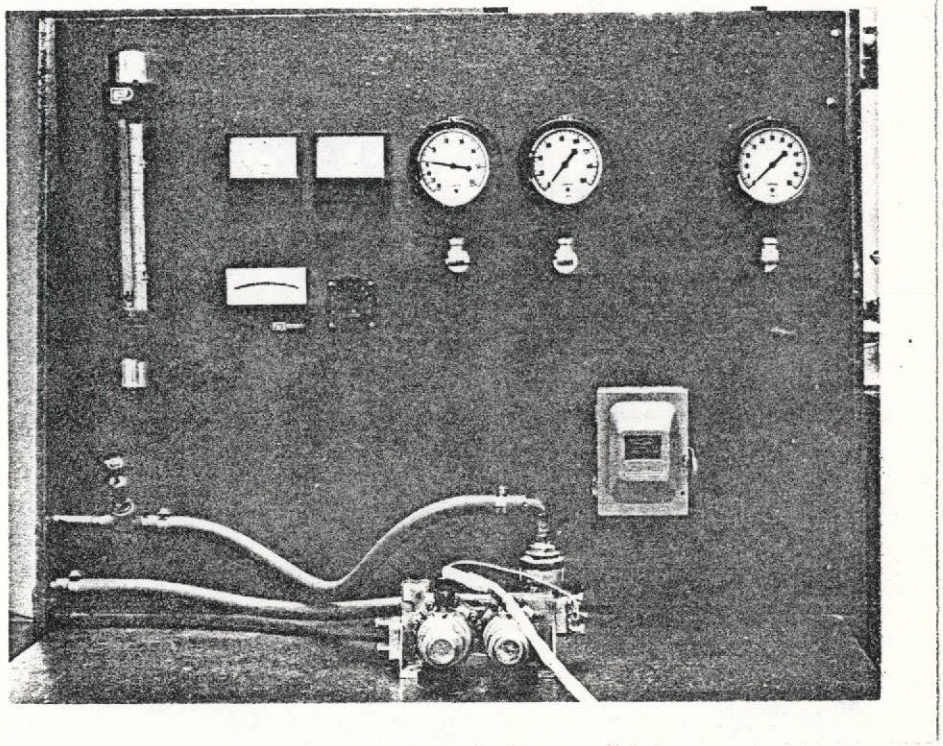

FIGURE 11 TEST BENCH WITH CENTRIFUGAL PUMP MOUNTED

condition. Input and output pressures and temperatures, as well as flows, were measured for each test. In addition, two high-frequency accelerometers were utilized for each test. The data from almost all tests were recorded on magnetic tape. Long endurance runs were not continuously taped, but samples were taped at intervals throughout the test. The data acquisition system is shown in block diagram form in Figure 12.

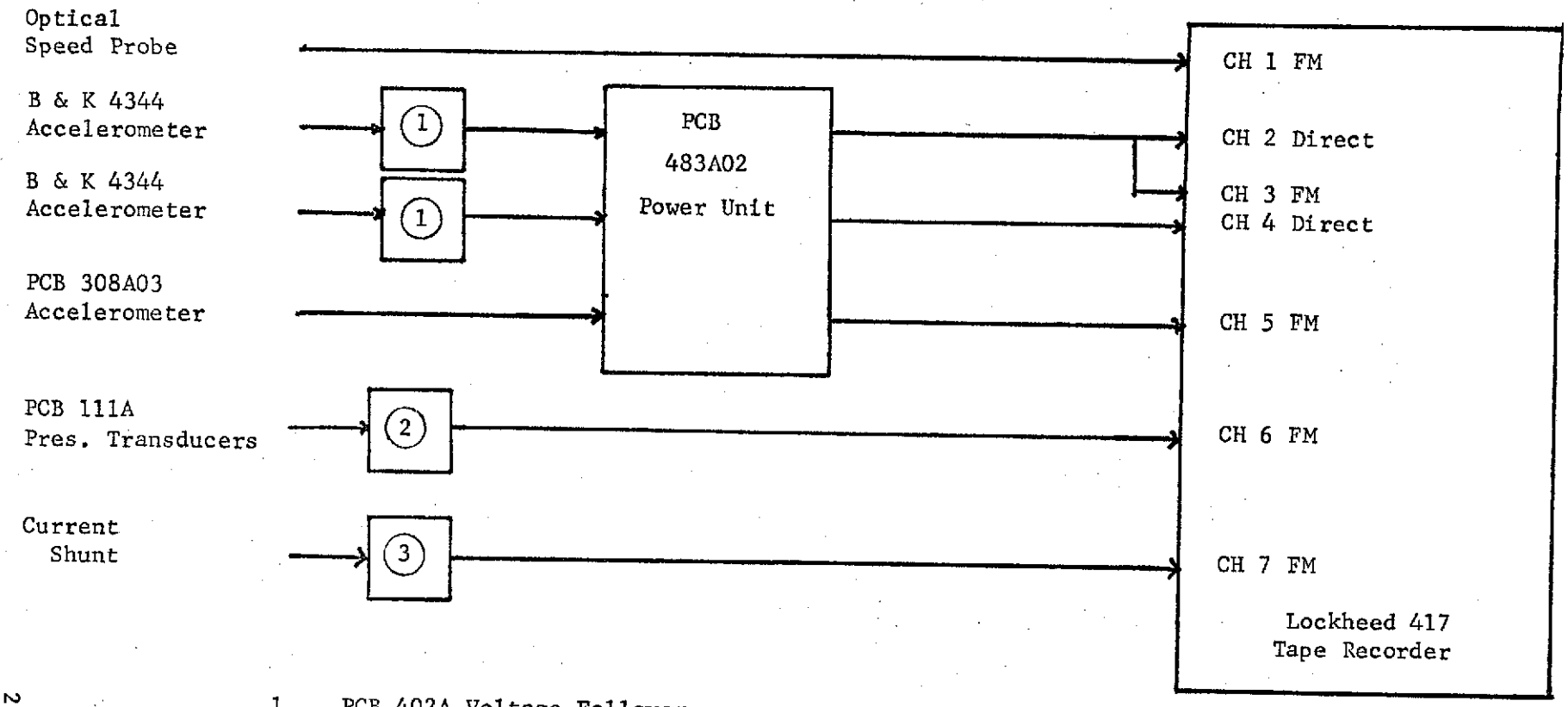

1. PCB 402A Voltage Follower
2. PCB 462A Change Amplifier
3. Encore 601 Differential Amplifier

FIGURE 12 DATA ACQUISITION SYSTEM

INITIAL TESTS — INTERNAL GEAR PUMP

Test Setup and Procedure

The testing conducted on the internal gear pump (Viking Pump Models FH432 and FH32) was designed to establish the character of signals generated by impacting components in the pump and to identify the trend in these signal characteristics as the pump was modified to simulate wear-out conditions that had been predicted for the pump. All tests were performed using the pump test loop described earlier.

Figure 13 is a closeup of the pump and shows the installation locations of the two high-frequency accelerometers, one low-frequency accelerometer mounted on the motor, and the dial indicator used to assure pump alignment and to induce known amounts of misalignment at the coupling.

The data recorded for each test is shown below.

Tape Channel	Record Mode	Measurement
1	F.M.	Motor Current
2	Direct	B&K Accelerometer #280 Pump Housing
3	F.M.	B&K Accelerometer #281 Input Shaft Housing
4	Direct	B&K Accelerometer #281 Input Shaft Housing
5	F.M.	PCB Accelerometer Motor Vibration
6	F.M.	Pump Discharge Pressure Dynamic Response
7	F.M.	Speed Signal 1/Rev

The tape recorder was operated at 30 ips, however, the F.M. electronics for 7 1/2 ips operation were used. This was done to reduce F.M. center frequency pickup on the direct channels. The frequency response of the direct channels was 200 Hz to 100 KHz. The frequency response of the F.M. channels was 0 to 2500 Hz.

Two basic reduction setups were used to analyze all pump data. These are shown in Figure 14 in block diagram form. Figure 14a simply uses the

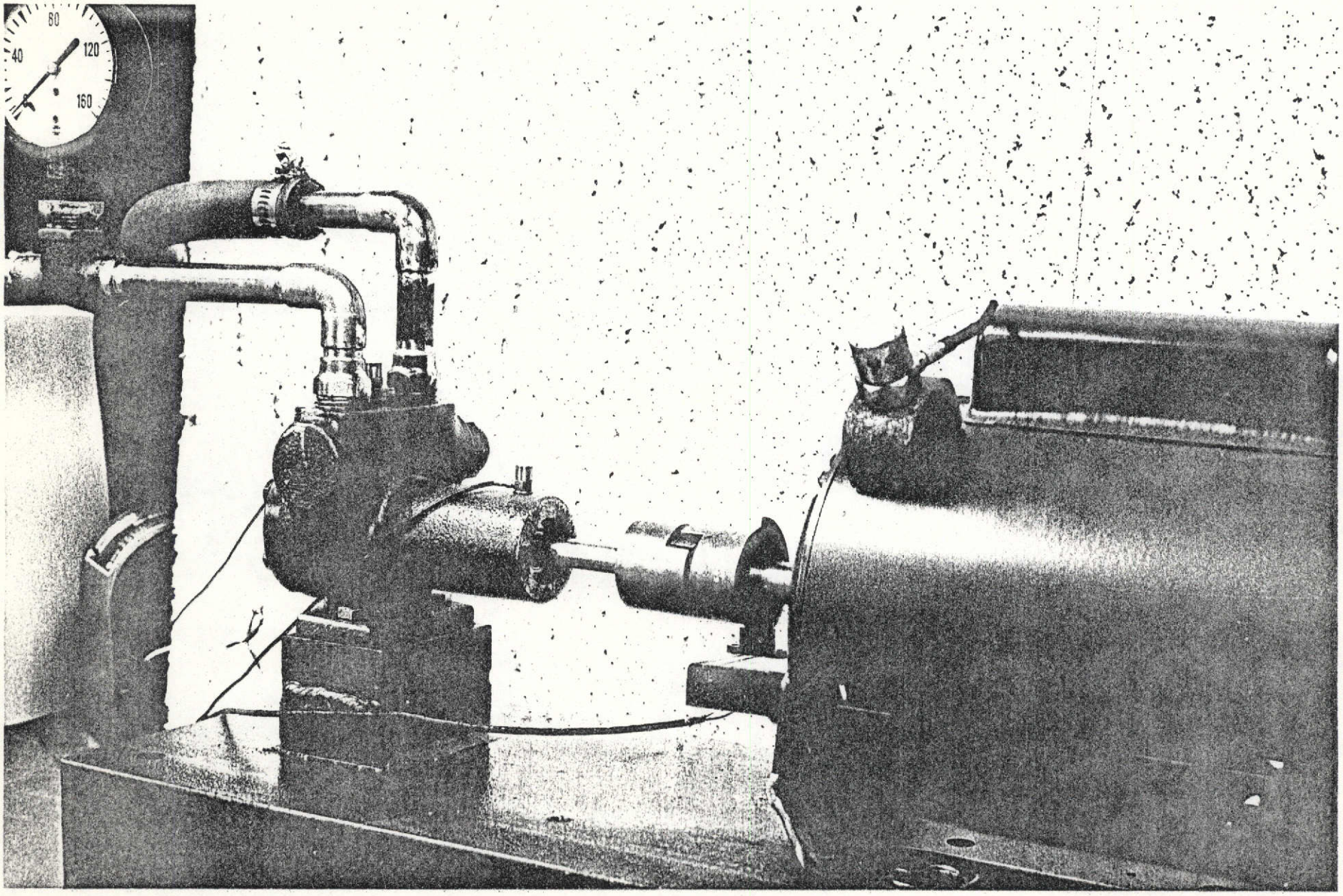

FIGURE 13 INTERNAL GEAR PUMP SHOWING TWO ACCELEROMETER LOCATIONS ON THE PUMP AND ONE LOW FREQUENCY ACCELEROMETER ON THE MOTOR

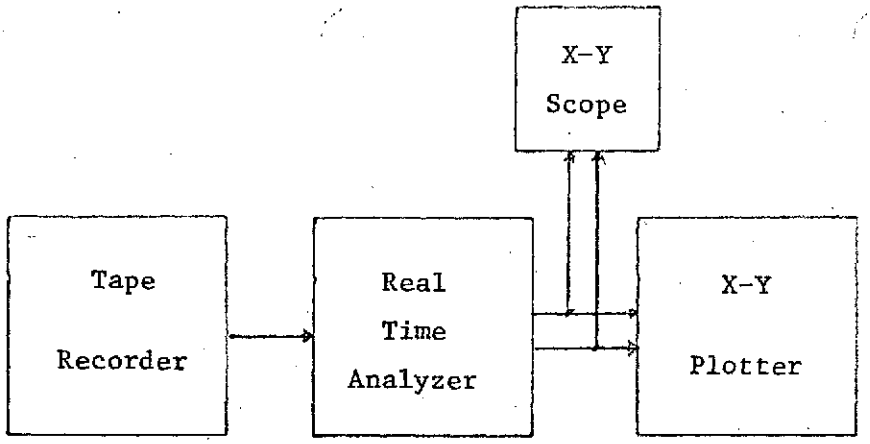

FIGURE 14a DATA REDUCTION FOR HIGH-FREQUENCY SPECTRA

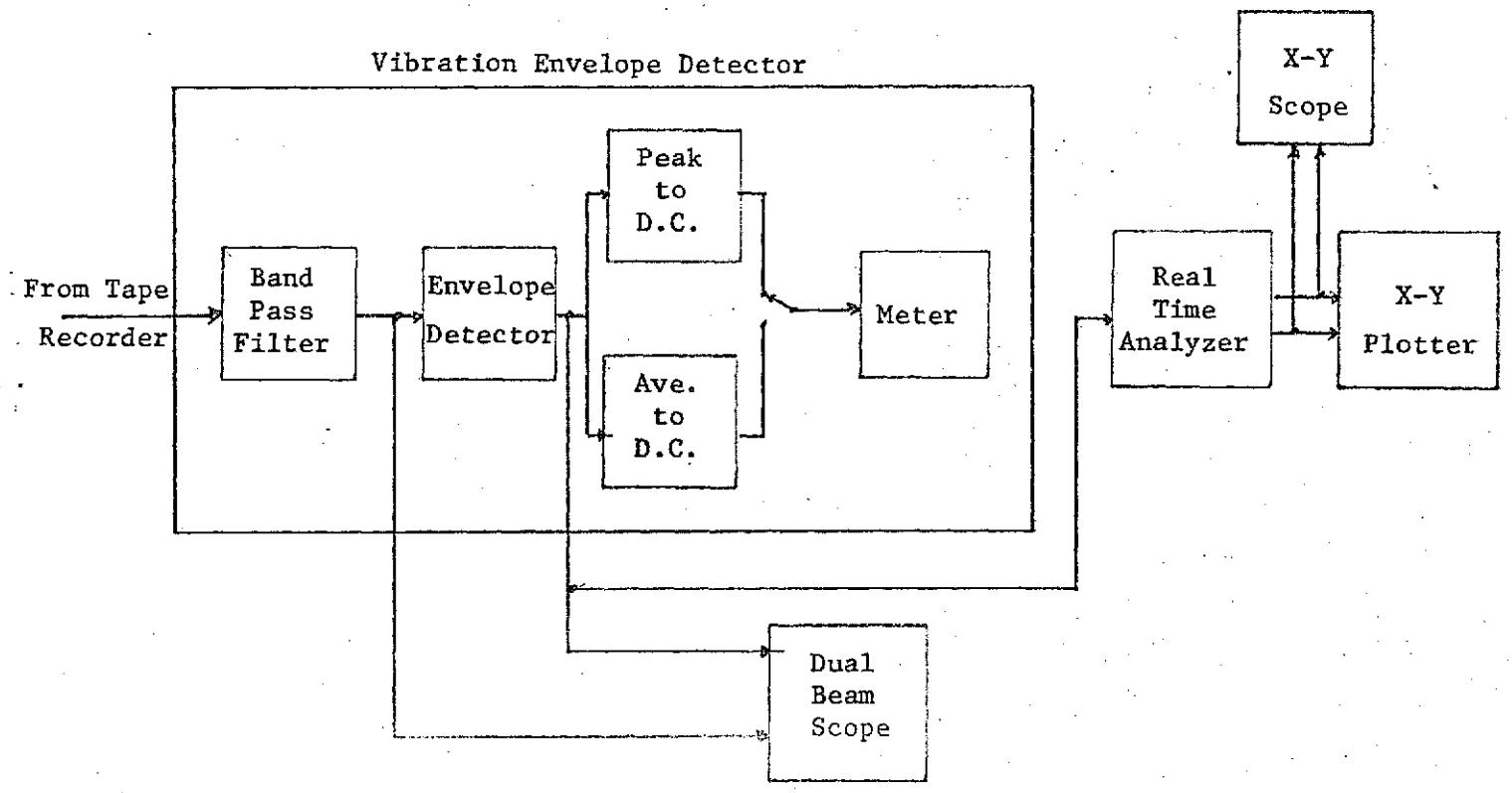

FIGURE 14b DATA REDUCTION FOR ENVELOPE CHARACTERISTIC IDENTIFICATION

FIGURE 14 DATA REDUCTION SETUP

real time analyzer to plot the spectra from 0 to 100 KHz. Typical data was shown in Figure 1. These data were analyzed to determine where the center frequency of the band pass filter should be set in the configuration shown in Figure 14b.

The analysis configuration of Figure 14b is used to produce scope pictures of the filtered and envelope-detected wave shapes and to plot the spectral content of the envelope-detected signal. Figures 2 and 3 presented earlier were produced in this manner. This data presentation is used to measure the peak amplitude of the impact. Figure 5 was a typical spectra of the envelope generated by the real time analyzer. Two spectra were run of each envelope: 0 to 100 Hz and 0 to 1000 Hz. The 0 to 100 Hz spectrum was used to get more resolution in the low-frequency region. The fundamental frequencies of interest for the Viking pump being driven at 1,780 rpm are as follows:

29.6 Hz	Input Shaft Speed, rps
42.0 Hz	Driven Gear Rotational Speed, rps
120 Hz	Motor Vibration
296 Hz	Gear Mesh Frequency
296 $\pm$ 29.6 Hz	Side Bands Due to Input Shaft Modulating Gear Mesh
296 $\pm$ 42 Hz	Side Bands Due to Driven Gear Rotational Speed Modulating Gear Mesh Frequency
296 $\pm$ 120 Hz	Side Bands Due to Motor Vibration Modulating the Gear Mesh Frequency

The spectra of the envelope shown in Figure 15 shows the presence of 29.6 Hz, 296 Hz, and 296 $\pm$ 29.6 Hz. This implies that the input shaft is rubbing, the gear teeth are impacting the pump casing, and that the amplitude of the impact is a function of the input shaft position. The last implication leads to the conclusion that there is cause and effect relationship between the input shaft rub and the gear teeth impacting the pump case. If the signals that appeared in the envelope-detected spectra were simply 29.6 Hz and 296 Hz, this would mean that the two phenomena were occurring independently.

The following tests were conducted on the Viking pumps:

1. Pump FH32 (packing seal) was run on a light oil over the full pressure and flow range.
2. Pump FH432 (face seal pump) was run on water in its as-new condition. The balance of the testing was conducted using this pump and on water. The pump was operated on water following each of the following modifications.

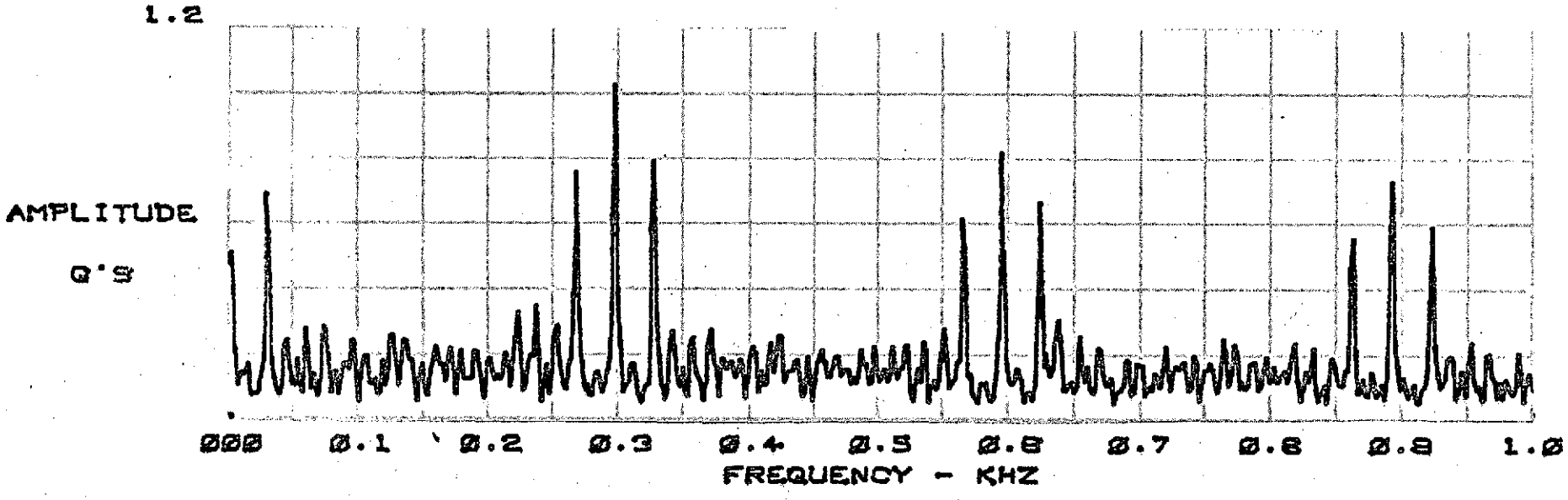

FIGURE 15 SPECTRA OF DEMODULATED SIGNAL - INTERNAL GEAR PUMP

3. The gear teeth were reduced in radius by 0.001 inches.
4. The gear teeth were reduced in radius by another .001 inches.
5. The carbon bushing on the input shaft was removed, cleaned, and reinstalled.
6. The carbon bushing was reamed to increase its bore by 0.002 in.
7. The idler gear was reamed to increase its bore by 0.002 inch.

For each of the above conditions the pump was started at 0 psi and then operated at intermediate pressures of 20, 40, and 60 psi before operating at 75 psi. The pressure was then reduced in the same steps to 0 psi. The pump-motor centerline was then misaligned by 0.010 inches and the same test repeated.

Data Analysis

For each test condition, the following data was reduced to hard copy at both 0 and 75 psi:

Spectral Plot	-	0 to 100 KHz
Spectral Plot (Demod.)	-	0 to 1000 KHz
Spectral Plot (Demod.)	-	0 to 100 KHz
Scope Picture	-	Filtered Resonance
Scope Picture	-	Demodulated Signal

Presently all this data in its original form is unwielding and one tends to get lost in the details, especially since gains were selected for each run that insured the data was not compromised by the system dynamic range. This results in different gains and thus direct, easy comparison is difficult. The data has been tabulated in Table 1. All the tabulated data is taken after the high-frequency signal had been filtered and demodulated. The amplitudes of frequency components were taken from the spectra while the Max Peak reading was taken from the scope pictures of the demodulated data. Selected hardcopy spectra are included as backup data in the Appendix A.

As noted earlier, the amplitudes taken from the spectra are about an order of magnitude below the Max Peak signal amplitudes. This is due to the fact that the energy shared between harmonics is strongly dependent on the shape of the impact. The spectral amplitudes should not be relied on, therefore, to determine the extent of the pump degradation but rather to identify the source of the problem. The Max Peak amplitude on the other hand is a sensitive indication of overall pump quality, however, it alone does not indicate the reason for the degradation. The two pieces of information must be combined in a logical format called a

TABLE I

	Frequency									Max Peak	Flow	% Reduction in Flow
	29.6	59.2	42	84	120	296	296 + 42	296 + 42	296 + 42			
New Pump 0 psi			.9g	1.5g		2.8g				36g	3.59	
New Pump 75psi			.6g	.4g		.4g				9g	3.195	
Tips Relieved .001" 0 psi			.15g	.5g		.4g				4.5g	3.53	1.7%
Tips Relieved .001" 75 psi	1.g		.2g	.2g		.4g				1.5g	3.13	2 %
Tips Relieved .002" 0 psi			.15g							1.5g	3.50	2.5%
Tips Relieved .002" 75 psi			.8g	.6g	3.29g	5g		1.2g	3.2g	24g	3.07	3.9%
Idler-Crescent 0 psi Repositioned						.1g				1.2g	3.58	.3%
Idler-Crescent 75 psi Repositioned	.1g		.2g			.7g				1.2g	3.12	2.3%
Bushing Bored 0 psi .002"	.2g		.3g			.8g				9g	3.53	1.7%
Bushing Bored 75 psi .002"	.6g	.6g	.8g	.8g		3g	.5g	1g		12g	2.75	13.9%
Idler Bored 0 psi .002"			4g			6g		3g		42g	3.48	3 %
Idler Bored 75 psi .002"			2g			3g		2g		90g	2.53	20.8%

symptom-fault matrix to determine the nature and severity of the defect. The symptom-fault matrix for the Viking pump is shown in Figure 16. Two types of relationships between faults can exist. For minor wear, two components can wear independently of each other. For example, idler shaft wear and gear/crescent wear can each wear in a somewhat normal manner. At some point, however, the rotational position of the idler will effect the severity of the gear crescent wear. When this occurs, the two frequencies are not independent and new frequencies appear that are indicative of this interdependence of the two phenomena. These new frequencies are called sidebands and are equal to the sum and difference of the two individual frequencies.

Figure 17 is a plot of the peak amplitude of the signal at both 0 and 75 psi for the test condition conducted. The amplitude of the signal at 75 psi after the gear tip was reduced by 0.002 inches is due to assembly errors. The next test point labeled "cleaned bushing" was simply disassembled, cleaned and reassembled. From the plot of the peak amplitude, the tabulated data showing the signals present and the symptom-fault matrix, the following conclusions may be reached about the pump for each operating condition and at 0 psi and 75 psi.

Pump FH32 (packing seal) operating in as received condition on light oil.

0 psi - The pump exhibits medium amplitude impacts (22 g). These impacts are due to an input shaft rub and gear teech rubbing the crescent. The two conditions interact since sidebands exist. The pump is wearing heavily at 0 psi.

75 psi - The pump exhibits low level impacts (9 g) and none of the important frequencies had any significant amplitudes. The pump is operating properly at this pressure with only low wear occurring.

Pump FH432 (face seal pump) operating on water in as-received condition.

0 psi - Moderate impacting occurring (36 g). The sources of the impacts are identified as the idler gear rotation and the gear teeth rubbing the crescent. No interaction between the two exist (no sidebands) so that wear of the idler shaft has not progressed to the point where the idler gear may move eccentrically with the support shaft. This operating point is producing heavy wear.

75 psi - Reasonably low (9 g) impacting occurring. The source of impact is the same as for 0 psi but lower in amplitude with no interaction between the causes. The pump is operating properly at this pressure with only low wear occurring.

Data Characters	Fault						
Peak Amplitude High And Demodulated Signal of Following Frequency	Input Shaft Bushing Crescent Wear	Gear Crescent Wear	Input Shaft/ Seal Rub Inducing Gear Crescent Wear	Idler Shaft Wear	Idler Shaft Rub Inducing Gear Crescent Wear	Misaligned or Locked up Coupling	Locked up Coupling Causing Gear Crescent Wear
Input Shaft	X						
Input Shaft Gear Mesh	X	X					
Gear Mesh		X					
Input Shaft Gear Mesh Gear Mesh ± Input Shaft	X	X	X				
Idler Shaft				X			
Idler Shaft Gear Mesh		X		X			
Idler Shaft Gear Mesh Gear Mesh ± Idler Shaft		X		X	X		
120 Hz (Motor Winding Vib)						X	
Gear Mesh ± 120						X	X

FIGURE 16 SYMPTOM-FAULT MATRIX

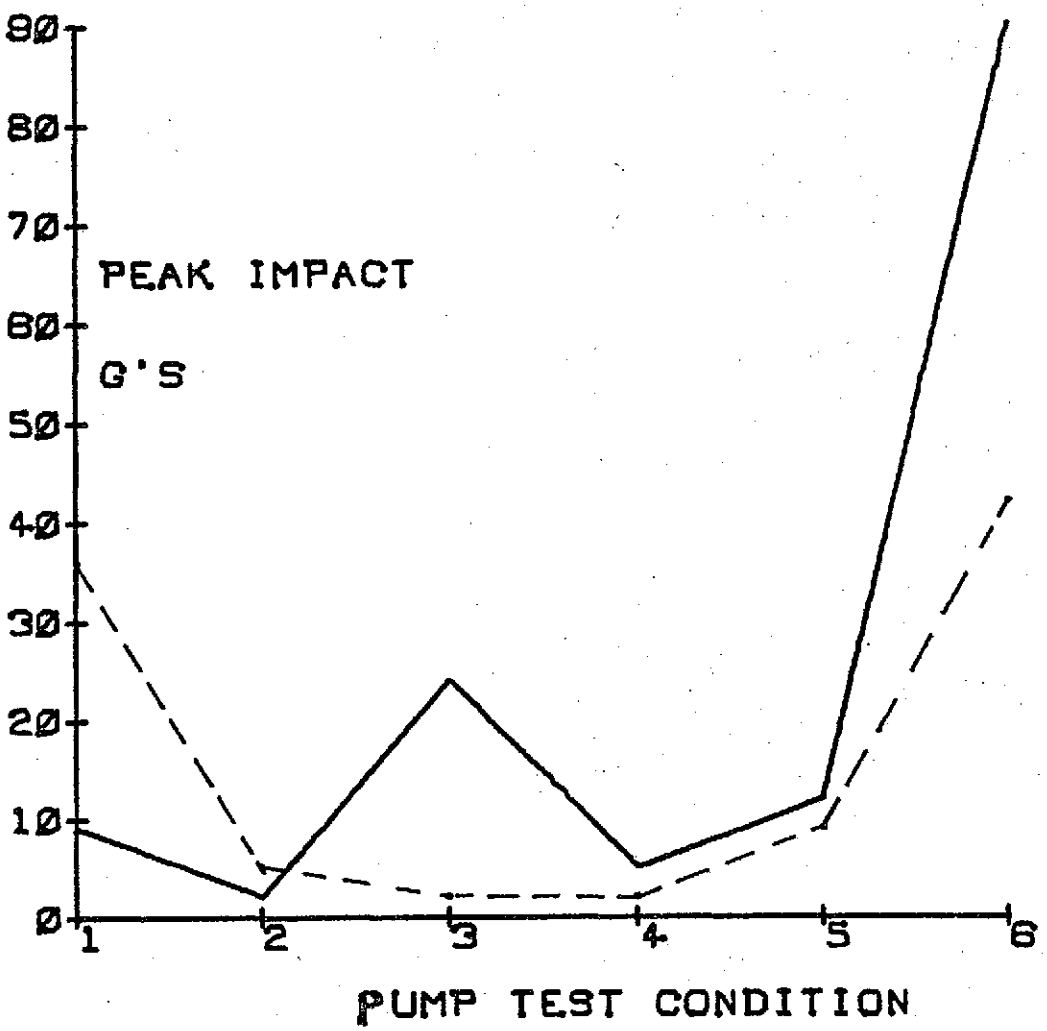

Pump Test Condition Key

1. New
2. Tips Relieved 0.001"
3. Tips Relieved 0.002"
4. Bushing Washed
5. Bushing Bored 0.002"
6. Idler Gear Bored 0.002"

FIGURE 17 PEAK IMPACT g LEVEL VS. PUMP CONDITION

Gear Tip relieved 1 mil.

0 psi - Low impacts occurring (4.5 g). Source is still the idler gear rubbing its shaft and the gear tip rubbing the crescent. Low wear occurring.

75 psi - Very low impacts occurring (1.5 g). The source is the same and signal levels are not low enough to detect some very low input shaft rubs. Low wear occurring at the test condition.

Gear Tip relieved further by 1 mil (two mils total).

0 psi - Very low impacts (1.5 g) occurring. Gear tips are not contacting the crescent. The only source is the idler gear rubbing its shaft. Very low wear occurring.

75 psi - Moderate impacting (25 g) occurring at any pressure over 0 psi. Sources of the impacting due to motor vibration (120 Hz), idler/shaft rubs, and gear teeth contacts with the crescent. There is low interaction between the idler/shaft rub and the gear teeth contact, however, very strong interaction exists between motor vibration and gear teeth contacts. Indication is that the pump has been improperly assembled and that the coupling is locked up allowing the shaft to transmit motor vibration. Heavy wear occurring.

Pump disassembled, small amount of residual kerosene material in input shaft bushing from manufacturer's test run. Bushing was cleaned and unit reassembled.

0 psi - Very low impact level (1.2 g) with only source minor contact between gear teeth and crescent. Almost no wear occurring.

75 psi - Slightly higher but still low level of impact (4.8 g). Sources of impact identified as input shaft rub, idler/shaft rub, and gear teeth contact with crescent. Minor wear occurring.

Carbon bushing on input shaft bored out by 2 mils to simulate wear of this component.

0 psi - Impact level still reasonably low (9 g), however, increased geatly from previous run. Source includes the input shaft due to increased clearance, idler/shaft rub, and gear teeth contact with crescent. Wear is light to moderate.

75 psi - Impact level is the highest (12 g) it has been at 75 psi except for incorrectly assembled pump and except for that point, this is the first time the impact level is higher at 75 psi than at 0 psi. Sources indicate both shaft rubs

and gear teeth to crescent rub. Additionally, all of these sources are interacting as shown by the family of sidebands. Wear is moderate.

The idler gear was bored 2 mils to increase the clearance simulating excessive wear of this component or the shaft.

0 psi - Moderate to heavy impacting occurring (42 g). Primary sources include the idler/shaft rub and the gear teeth to crescent rub. Strong sidebands indicate a great deal of interaction between the idler/shaft rub and the teeth/crescent rub.

75 psi - Heavy impacting occurring (90 g). The same sources and interaction is expected since as the gear moves on the shaft, the gear teeth are allowed to contact the crescent. Heavy wear occurring.

FINAL TESTING - INTERNAL GEAR PUMP

A question naturally arises as to how the type of signals obtained from simulating wear on critical components would compare against those types of signals generated by an unmodified pump naturally wearing or that was in distress. In order to investigate this point, a new internal gear pump of the same design as used for the initial testing was mounted on the test bench in exactly the same manner as the initial unit (Figure 13). Pump pressure was set for 85 psi. The overall g level of the signal from the pump accelerometer was 600 g's peak. Since this is 6 to 7 times the worst amplitude in the initial tests, the conclusion was that the pump had already failed; or, more precisely, was in danger of imminent catastrophic failure.

The definition of failure now needs to be defined for this positive displacement pump. The criteria suggested in the contract work statement that the time of pump failure can be considered to be when the pump operational parameters, pressure, and/or flow have been reduced by 15 percent. Analysis of the Viking pump and how it fails have led to another criteria for failure. Motor current was selected and the failure point was set as that point when the motor current had increased by 15 percent. The reason for not selecting flow, for example, results from the manner in which this pump can be expected to wear out. The Viking pump is a positive displacement pump, therefore, flow is first a function of pump speed and secondly a function of internal leakage in the pump. Leakage could be a function of pump wear, however, an analysis of the pump shows that the pressure holds the idler gear against the crescent and therefore tends to compensate for wear. It was observed that, depending on the severity of wear, the pump could slow down and thus the flow would drop off. This, of course, would depend on the power rating of the motor chosen and not on the pump or its condition. From the above it can be seen that flow variation is not directly related to pump condition but rather to additional factors not directly related to pump condition. Regardless of the size of the motor used, if the wear becomes heavy in the pump, the torque required to turn the pump goes up and thus the current must go up. Final catastrophic failure of the pump/motor combination will occur when the pump seizes or the current requirements of the motor exceeds its rating or the rating of the protective fuse.

To check the conclusion that the pump had failed, it was disassembled and examined. The gear teeth and the crescent were heavily galled from just a short run. The current during the initial run approached 10 ampheres versus a normal current for 75 psi of 7.5 to 7.7 amp. This was a 30 percent increase in current. The pump was reassembled and operated again at 75 psi with the same results. At this point, the pressure was

reduced. At 30 psi the peak g level, as read by the vibration envelope detector, had fallen to almost 0 g's. Forty hours later the level had reached 200 g's. The peak g levels are plotted versus time (not linear) in Figure 18. If the pump were shut down as it was over the weekend after 40 hours of running, the starting g level increased to 350 g then rapidly dropped to the previous level. During this period, the pump current stayed within its normal range.

The level of 200 g's at the time seemed high (when compared to earlier 92 g peak and the damaging 600 g), however, subsequent running proved that the pump would easily operate for 300 hours at these signal levels. On the basis of this experience, the limit appears to be approximately 400 to 500 g's; however, the lower of these figures would probably be the prudent choice. A double check on this value is provided by the fact that the current did not become excessive.

The pump was removed after 448 hours of operation. Approximately one week later the pump was returned to the test stand. When operated at 30 psi, a peak g level of 120 g's was recorded which by previous experience would assure another 300 hours of successful operation. There seemed little value in operating another 300 hours at 30 psi. The decision was then made to try to operate at the higher pressures which was impossible earlier. Figure 19 shows the result of four attempts to raise the pressure to 80 psi.

The first attempt to run at 80 psi was terminated when the peak g level (of the high-frequency resonance) reached 1,000 g's. After returning to 30 psi, the g level continued to decrease to below previous values; indicating that at this pressure the pump was operating better than before. Next followed two almost identical cycles. The pressure was raised to 80 psi while the peak g level decreased to almost zero. Within an hour, however, the peak g level was back at 1,000 g's. In each of these cases the current also went up to over 10 amp. The fuse was shorted to allow operation at over 10 amp.

The fourth attempt to reach 80 psi resulted in the g level again dropping to almost zero. Instead of climbing to 1,000 g's, however, the g level had only reached 90 g's twenty four hours later. Motor current was normal.

Since this g level was stable and below the level of 400 g's, it was predicted that the unit should operate at this pressure for three hundred hours. Figure 19 shows the operation for approximately 500 hours which substantiates the detection criteria.

The variations in vibration levels may appear on the surface as rather unusual. If, however, it is recalled that increasing discharge pressure increases loads of both gears against the idler, it would be anticipated vibration levels that would increase with pressure. When

gauling was encountered between gears and crescent, vibration levels exceeded 500 g's. The pressure could then be reduced to a level where gauling did not occur and only burnishing type wear was encountered and g levels would drop. During this operation, the gauled areas would tend to burnish-in. Higher pressures could then be repeated with reduced vibration levels until gauling would again occur. During the fourth attempt to run at 80 psi, the burnishing type wear continued without gauling and vibration levels dropped to the 90 g level.

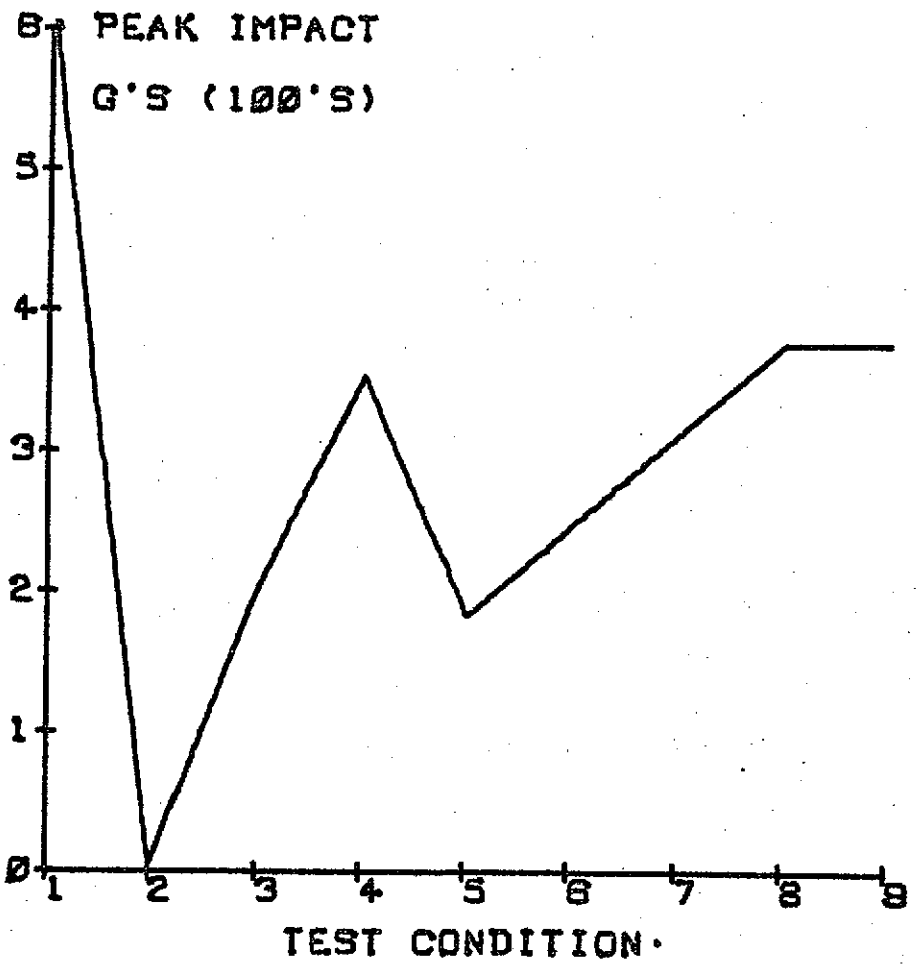

Test Condition Key

1. 75 psi Operation - New Pump
2. 30 psi - 0 Hours
3. 30 psi - 40 Hours
4. Start After Weekend - 40 Hours
5. Recovery - 40 Hours
6. Endurance Run
7. Endurance Run
8. Endurance Run - 320 Hours
9. End of Test - 448 Hours

FIGURE 18 ENDURANCE TESTING AT 30 psi

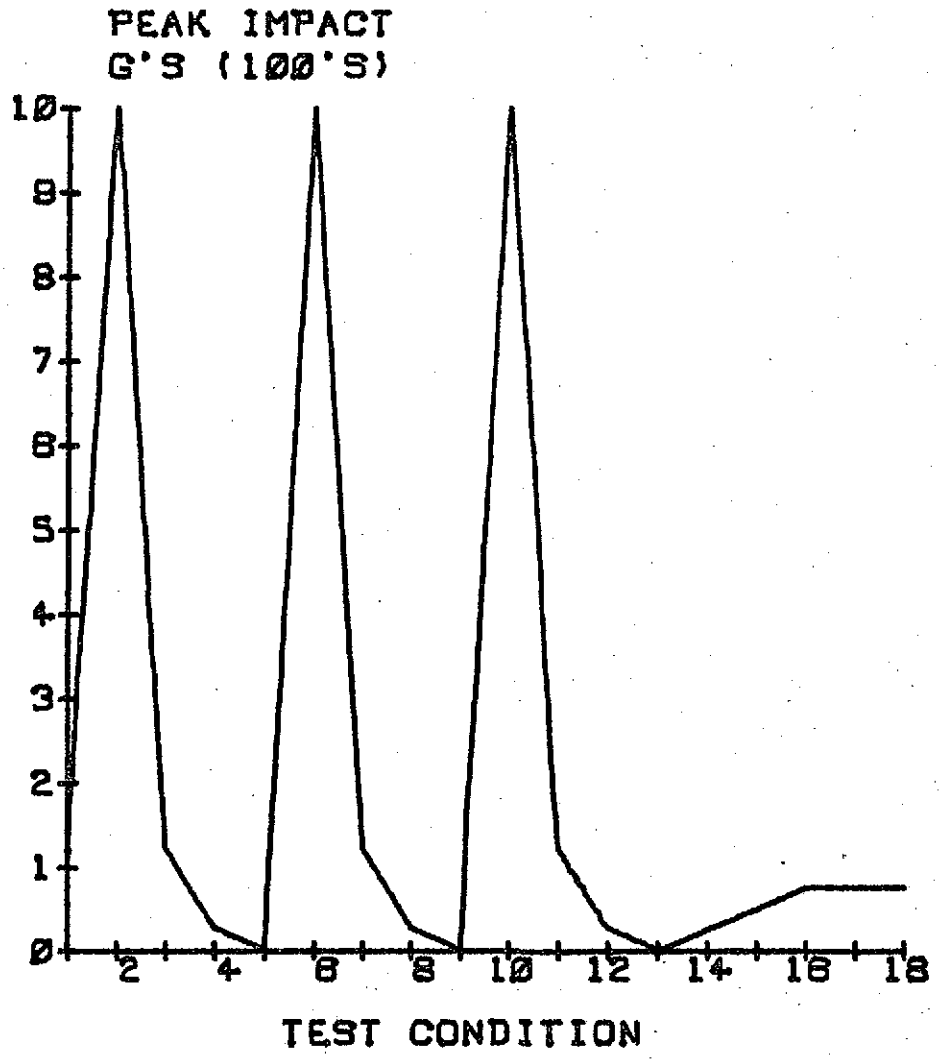

Test Condition Key

1.	30 psi - Operating	10.	80 psi - 45 Minutes Later
2.	80 psi - Test	11.	30 psi
3.	Return to 30 psi	12.	30 psi - 5 Hours Later
4.	30 psi - 5 Hours Later	13.	80 psi
5.	80 psi	14.	80 psi - 12 Hours Later
6.	80 psi - 45 Minutes Later	15.	80 psi - 24 Hours Later
7.	30 psi	16.	80 psi - Start of Endurance
8.	30 psi - 5 Hours Later	17.	80 psi - 250 Hours
9.	80 psi	18.	80 psi - 500 Hours

FIGURE 19 BREAK IN PROCEDURE AND ENDURANCE TESTING AT 80 psi

INITIAL TESTING - CENTRIFUGAL PUMP

As described earlier, the centrifugal pump (AiResearch #580745-1-1) was a dual-pump unit consisting of independent motors and pumps in one overall housing. The pump had been used at NASA-MSFC for endurance testing and there was no reason to believe that the pump was not in excellent condition. The pump operates on three-phase, 400 Hz power; and a 28 V to 400 Hz three-phase inverter was furnished along with the pump. One side of the pump was disassembled at Shaker Research and inspected. This side of the pump was labeled SRC. The side that was not disassembled but run in its as-received condition was labeled NAS.

Both pumps were operated with accelerometers mounted on the motor and on the pump. Figure 20 shows the typical accelerometer locations. Figure 1 shows the typical high-frequency spectra obtained during these tests. Note the g levels for these signals are extremely low when compared to the positive displacement internal gear pump. Table 2 lists the high-frequency resonances detected for each accelerometer location for each pump.

TABLE 2

SRC Unit		NAS Unit	
Pump	Motor	Pump	Motor
18 KHz	18 KHz	18.4 KHz	16.8 KHz
35 KHz	28 KHz	34.2 KHz	25.8 KHz
57 KHz	37.6 KHz	50.4 KHz	35.2 KHz
67.4 KHz	57 KHz	67.2 KHz	55.8 KHz
	68 KHz		65.8 KHz

Each resonance was examined in the following manner (refer to data reduction block diagram, Figure 14):

1. Spectra, 0 to 1000 Hz, of the envelope of each of the resonances identified above were produced. These spectra were at the 1.5 gpm flow condition.
2. The discrete signals in the envelope spectra were identified.
3. On the basis of the identified discrete signal components, a decision was made as to which resonance provided the clearest definition of a given defect signal.
4. Each of the resonances identified in 3 (above) were then

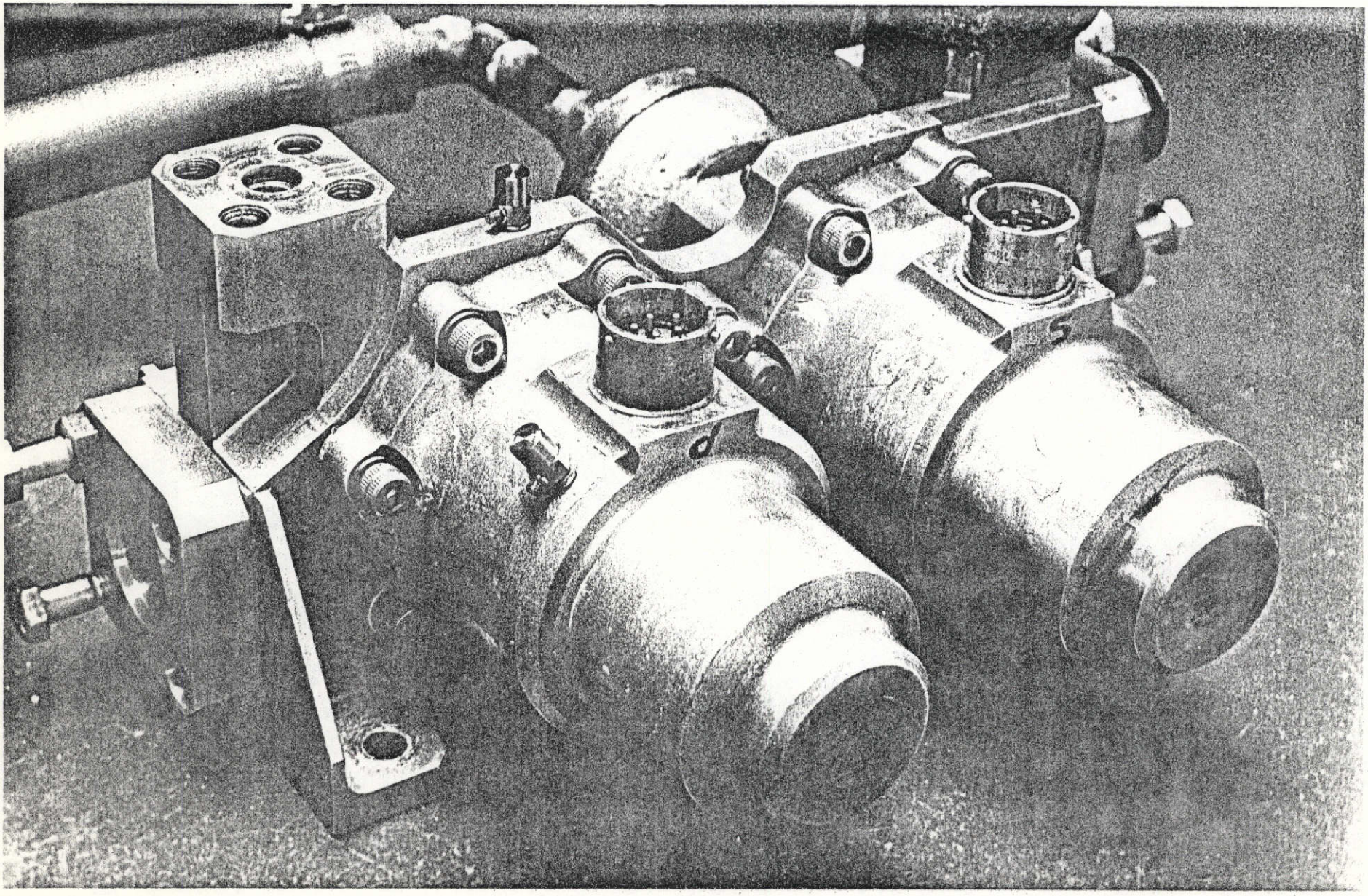

FIGURE 20 CENTRIFUGAL PUMP SHOWING THE TWO ACCELEROMETER LOCATIONS

analyzed at each flow point.

5. The amplitudes of the defect-related signals were tabulated.

This procedure, while utilizing the real time analyzer, could be duplicated by using the pump failure anticipator design submitted. The low-frequency band pass filter needed to perform the analysis had not been breadboarded and, therefore, was not available.

Detailed spectra that were plotted at this time are shown in the appendix. Initially, three resonances were selected for further analysis in step 3, above, these were:

28 KHz - motor
55 KHz - motor
35 KHz - pump

The resonance located at approximately 65 KHz was not used since it is likely that it could be due to the accelerometer mounting and not a structural resonance of the pump. This fact was investigated by mounting the accelerometers to the blocks and gluing them back to back. One accelerometer was excited by an oscillator and resonances were identified by observing the lissajous figure on the scope. The resonance at 65 KHz was confirmed to be due to the mounting blocks, however, the 55 KHz resonance was also identified as due to the method of mounting. Therefore, both the resonances at 55 KHz and 65 KHz were discarded from further consideration. This conclusion was verified in the final testing when the mounting method was changed and the 55 KHz and 65 KHz resonances disappeared. It is important to reject accelerometer mounting resonances, even when large signals can be obtained, since any variation in mounting procedures can have large effects on signal repeatability.

The resonances that remained of interest were the 28 KHz resonance on the motor and the 35 KHz resonance on the pump. In the demodulated data, the frequencies of interest are the bearing defect signals caused by an irregularity on the inner and outer race or on the rolling element, the once and twice per rev and the signals related to the power frequency (1/2 f, f, 2 f). The 1/2 f is of interest if the motor is a four-pole motor as it is on the AiResearch pump drive motor.

The mechanically-related signals were calculated and are plotted versus pump speed in Figure 21. In the initial operation of the pump, the D.C. to 400 Hz inverter was powered by 25.2 volts rather than the rated 28 V. This resulted in speed and electrical variation versus flow as shown in Figure 22. The final testing on this pump used the proper D.C. voltage and the speed and frequency were much more stable.

The amplitude of each of the discrete defect signals appearing in the high-frequency resonance (28 KHz and 35 KHz) was tabulated for each

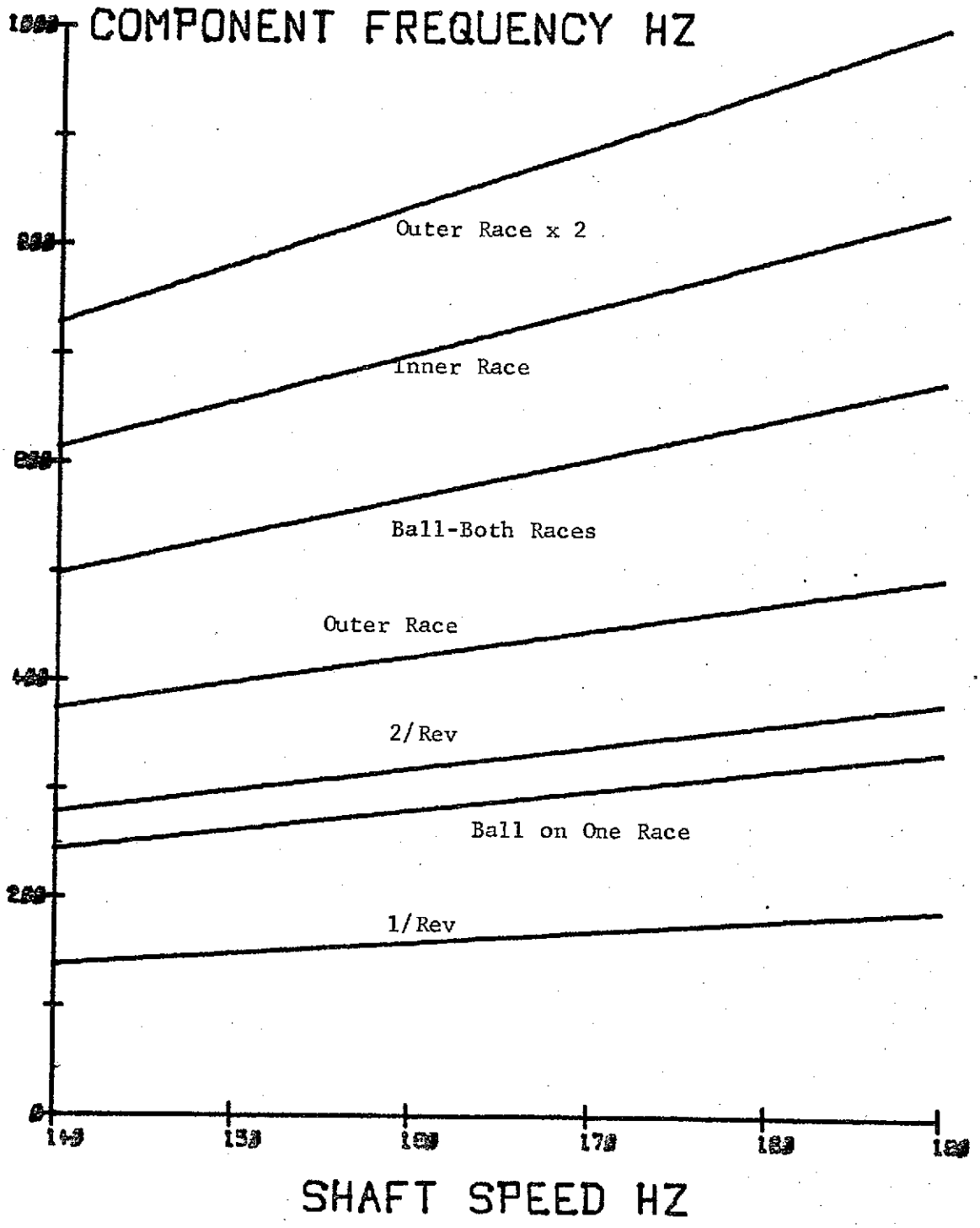

FIGURE 21 COMPONENT DEFECT SIGNAL FREQUENCY VS. PUMP SPEED

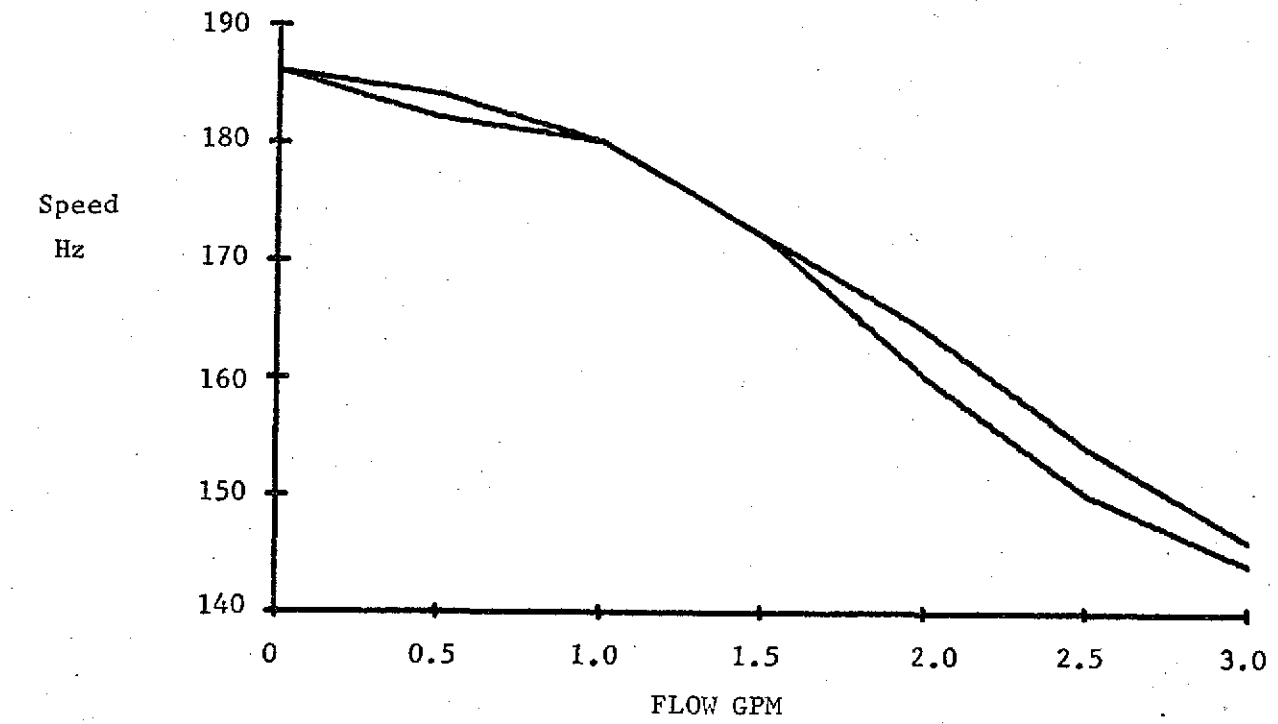

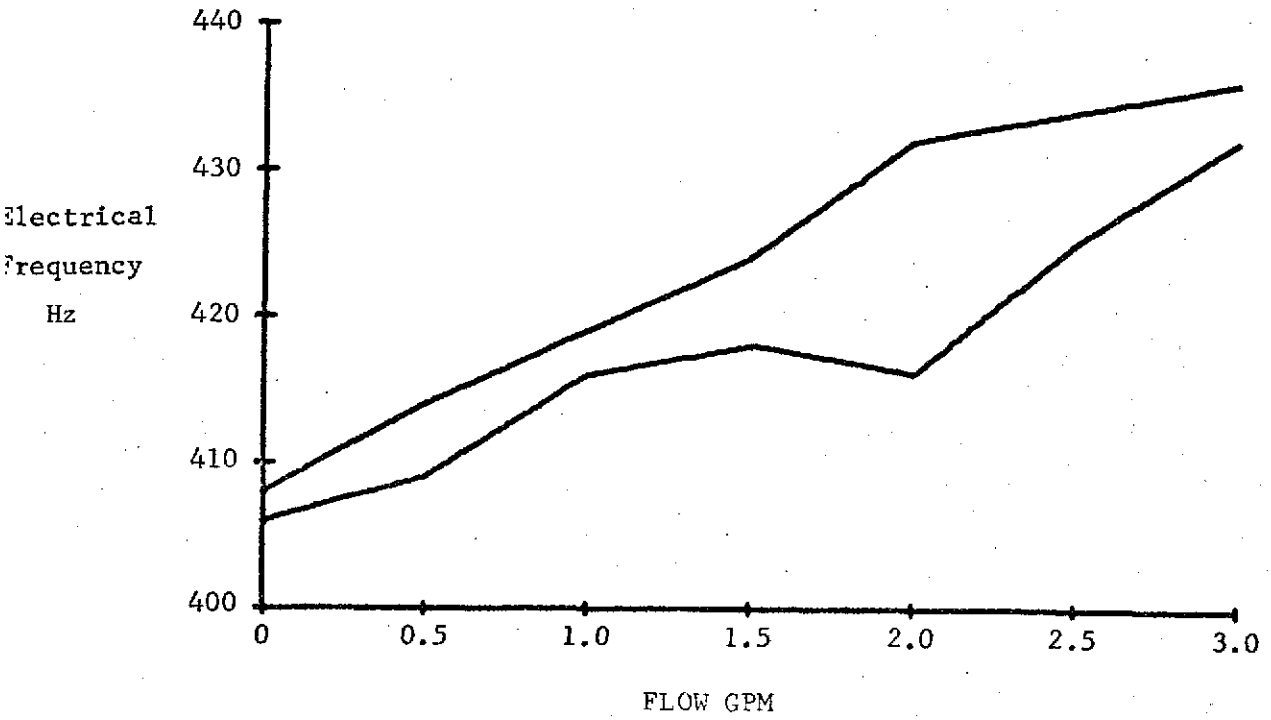

FIGURE 22 SPEED AND ELECTRICAL FREQUENCY VS. FLOW

pump. This tabulation is shown in Table 3. The values shown in this table may be obtained by noting the peak amplitude of the spectral component in the appropriate spectra in Appendix B. The following initial conclusions may be drawn on the condition of the two pumps.

Motor Ball Bearing

SRC Unit - Very low signal in the 54 KHz resonance and no signals present in the 28 KHz resonance. Conclusion: bearings in excellent condition.

NAS Unit - Low level but existent signals for ball and outer race defect. Medium level signal for inner race. Conclusion: bearing has a minor defect on the inner race.

Motor Windings

Both the SRC and NAS units had the same amplitude 400 Hz signals. The conclusion is that both motors are in an as-new condition since it is unlikely that two motors would degrade identically.

Pump Journal Bearing

Both the units had low-level, once-per-rev signals. Conclusion: neither shaft is rubbing the journal.

The results of these tests indicated that the high frequency vibration technique was suitable to detect pump faults that would lead to pump failure. Although life tests were not run on these pumps, the frequency ranges were identified where stress in the pump would be discerned. It appeared reasonable that levels could be established with additional testing, to indicate impending failure well before the failure occurred.

	SRC					NAS				
FLOW PGM	BEARING g's			ELECTRICAL g's	PUMP g's	BEARING g's			ELECTRICAL g's	PUMP g's
	BALL	IR	OR			BALL	IR	OR		
0	--	--	--	.03	.08	.08	.18	--	.03	--
0.5	--	--	--	.05	.1	.07	.17	--	.07	--
1.0	--	--	--	.1	.08	.06	.15	--	.07	--
1.5	--	--	--	.14	.05	.05	.12	--	.14	.02
2.0	--	--	--	.03	--	--	.08	--	.1	--
2.5	--	--	--	.03	--	--	--	--	.03	--
3.0	--	--	--	.03	--	--	--	--	.05	--

TABLE III DEFECT SIGNAL AMPLITUDES - INITIAL TESTS CENTRIFUGAL PUMP

VIBRATION ENVELOPE DETECTOR (PUMP FAILURE ANTICIPATOR)

The block diagram for the engineering model Vibration Envelope Detector (VED) is shown in Figure 23. Four sets of data are shown that characterize the signal at four different points in the circuit and also relate to examples of data processing previously discussed. Three of these sets show both the frequency and time domain signals while the output of band pass filter B is an almost pure tone shown only in the time domain.

The block diagram as shown in Figure 23 is the most versitile. Data obtained to date indicates that possibly not all blocks would be required in the final unit and that some controls and outputs could be eliminated to simplify the operation, however, for the present program, the maximum sensitivity shown was retained. The example of the processed data in Figure 23 are for the switch portion shown. The description of the block diagram follows:

There are two inputs to the unit--one labeled accelerometer input and one voltage input.

When the VED is used on a pump in real time, the accelerometer mounted to the pump is connected to the charge amplifier which conditions the data (removes effect of cable capacitance) and normalizes it to take into account different accelerometer sensitivities. If magnetic recordings of data obtained during pump tests are made, this type of data is played back into the volt in input and bypasses the charge amplifier. At the next stage in the unit, either a low pass or a hi pass filter may be inserted or both filters bypassed. If the data to be analyzed has high amplitude signals not in the range of interest (either high or low frequency), then the proper filter is selected to reject the signal so that the maximum dynamic range of the unit may be employed for the signals of interest. The lo pass filter would be used only when low-frequency vibration signals are of interest. In this case, the high-frequency band pass filter A and the envelope detector would be bypassed and the system would act as a low-frequency band pass filter.

In the data shown in Figure 23 for the first output point, the low-frequency component is smaller than the high-frequency component of interest and there is no need to reject the low-frequency signals since they will be rejected by band pass filter A and their presence in the amplifier does not significantly reduce the system dynamic range. The low-frequency component present in the time domain data for the input obscures the presence of the impact-excited, high-frequency vibration, as can be seen by comparing the signal after the high-frequency band pass filter.

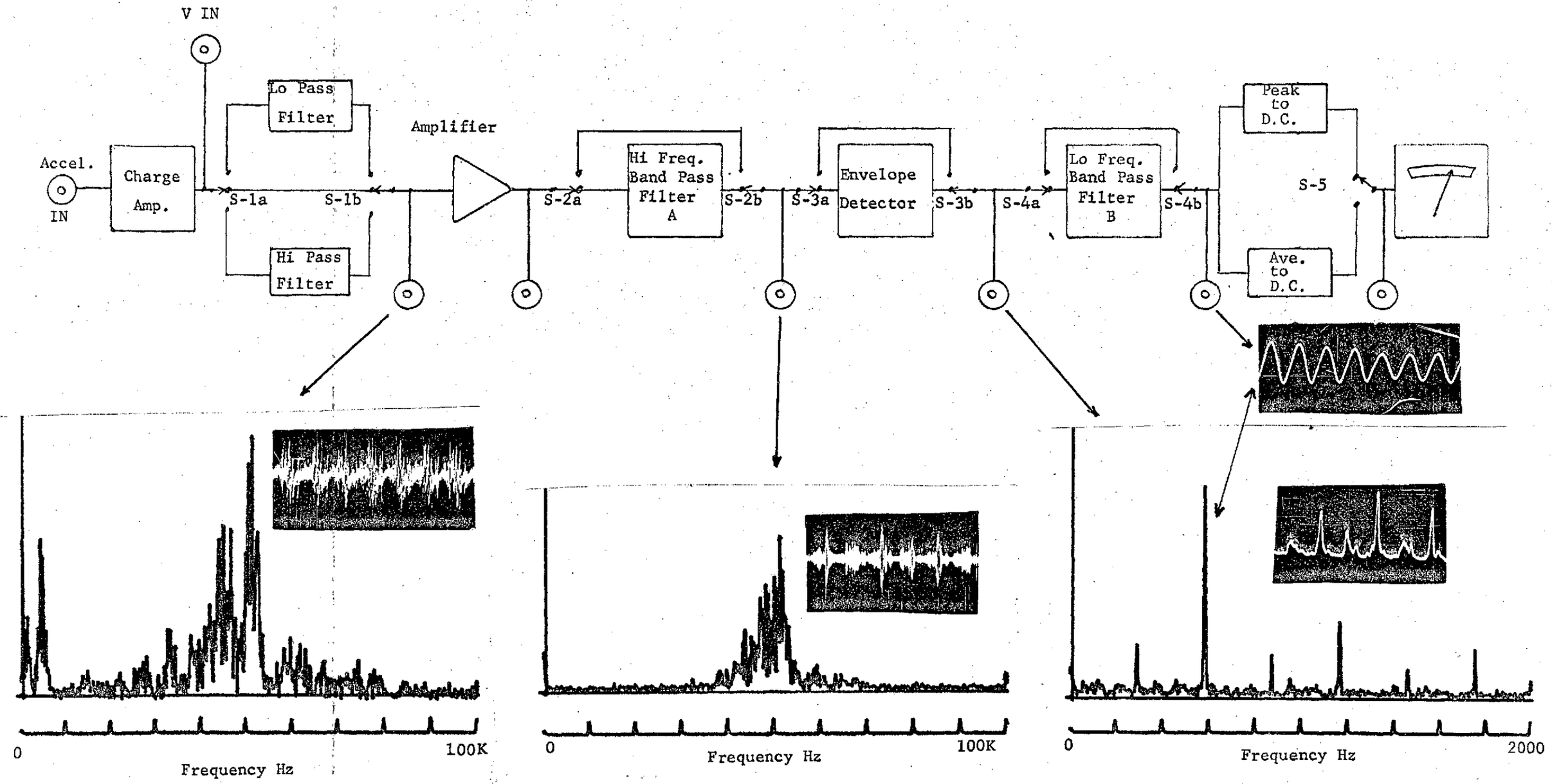

FIGURE 23 PUMP FAILURE ANTICIPATOR BLOCK DIAGRAM AND SIGNAL FLOW

FOLDOUT FRAME

FOLDOUT FRAME

The amplifier has fixed gain set with no vernier control. This is done to preclude the possibility of operating the unit in an uncalibrated mode. High-frequency band pass filter has been set so that its center frequency is 50 KHz. The Q of the filter is 10 and, therefore, begins to attenuate signals outside of a pass band 5 KHz. The major source of the impacts shown in the data at the band pass filter output (Figure 23) is due to a chattering relief valve. The chatter rate has synchronized itself with the second harmonic of the gear mesh signals. The gear impact signal may be seen as the sharp rise time signal occurring every other pulse. The relief valve contribution may be seen in every pulse.

The envelope detector produces the data shown in the third set of data (Figure 23). The time domain signal as observed on oscilloscope follows the envelope of the positive half of the filtered signal. The frequency content of the signal may be determined by performing a spectral analysis of the envelope wave form. The gear mesh signal fundamental (from the internal gear pump) is the signal at 294 Hz. It can be seen that the second harmonic at 588 Hz is the predominant component. The same information can be determined by tuning the low-frequency band pass filter to each component and reading the relative amplitudes on the meter. The filtered wave shape is shown in the fourth time domain photo. The band pass filter rejects the D.C. level of the envelope so that the average value of any signal passing through the low-frequency band pass filter is zero. All amplitude readings made after this filter must, therefore, be done in the peak mode.

On the internal gear pump used in testing to date, the frequencies of interest are 29 Hz, rotational speed of input shaft at the carbon bushing, 42 Hz, rotational speed of the internal gear on its journal bearing and 294, the gear mesh signal. The harmonics of each signal are also of importance. These low-frequency signals are not present or very low in the frequency spectrum but are contained in the envelope of the high-frequency resonance. Figure 24 is a photo of the completed system. Figure 25 shows the card layout and construction of the system.

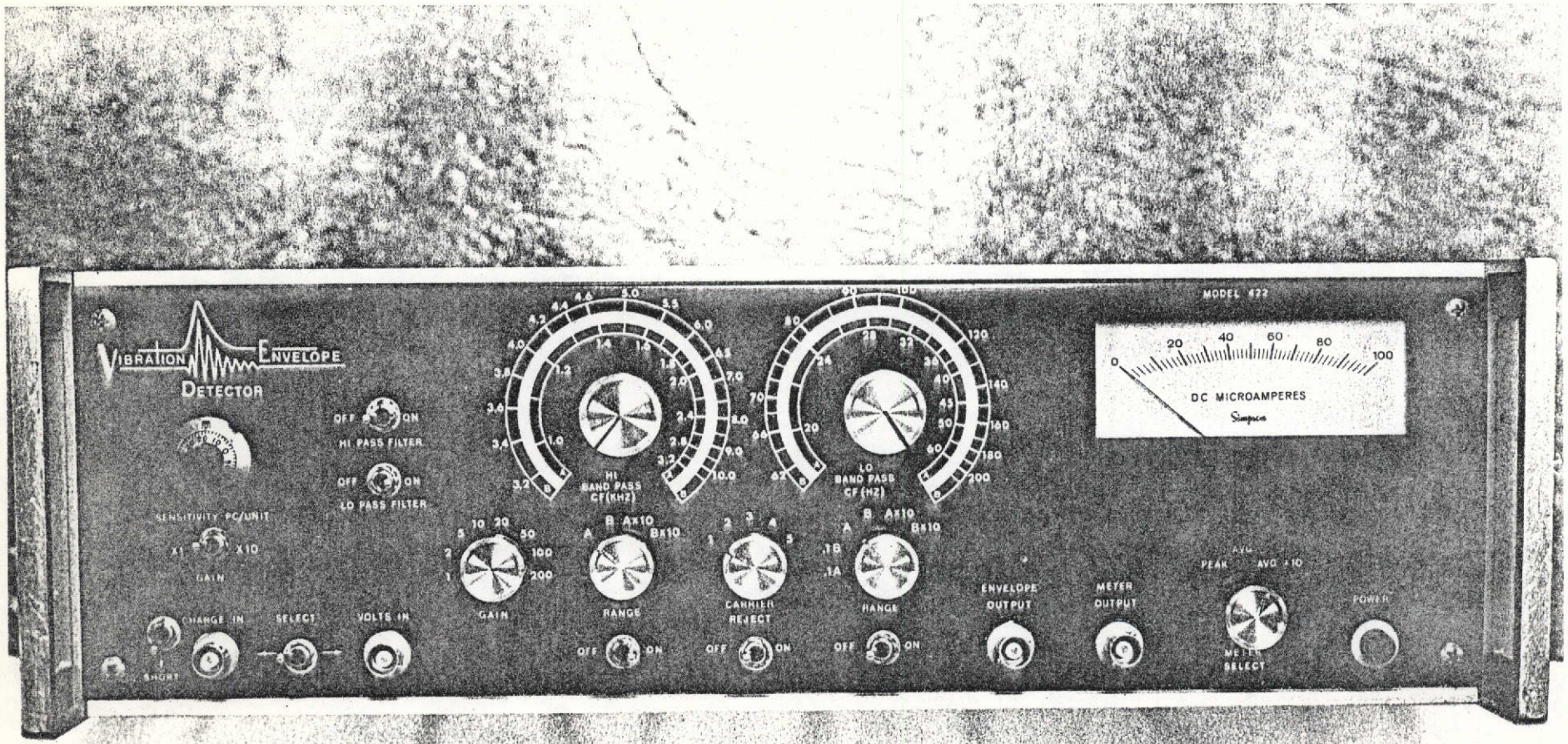

FIGURE 24 FRONT PANEL OF THE VIBRATION ENVELOPE DETECTOR

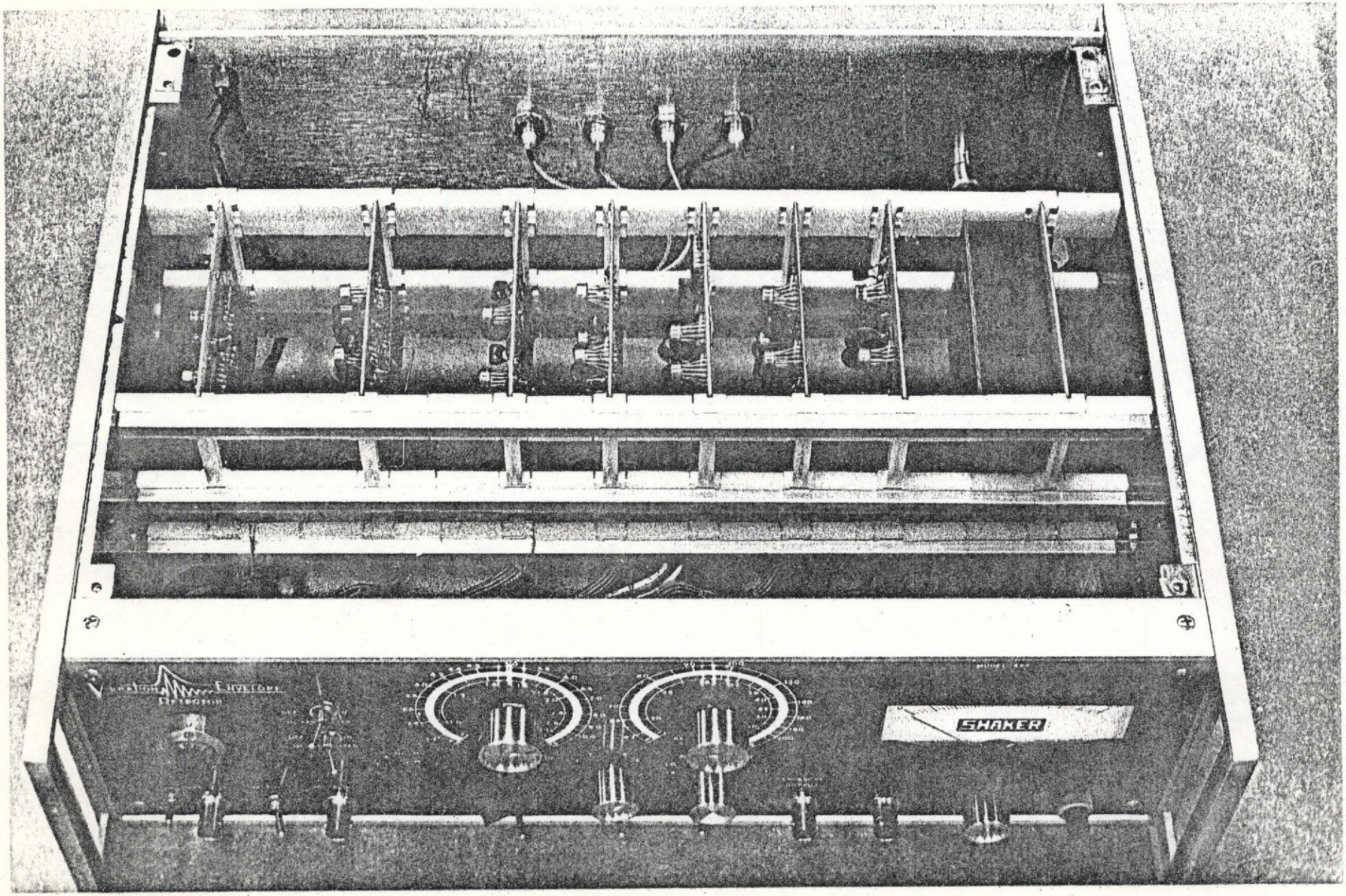

FIGURE 25 VIBRATION ENVELOPE DETECTOR WITH PROTOTYPE CARDS. CARDS FROM LEFT TO RIGHT ARE; 1) CHARGE AMPLIFIER; 2) LOW/HI PASS FILTER; 3) AMPLIFIER; 4) HI FREQUENCY BAND PASS FILTER; 5) ENVELOPE DETECTOR; 6) LO FREQUENCY BAND PASS FILTER; 7) PEAK/ARC DETECTOR; AND 8) THE POWER SUPPLY.

VERIFICATION TESTS

Test Procedure

The AiResearch pump has been described along with the most important failure modes of the pump. These failure modes were as follows:

Motor - ball bearing brinnelling
ball bearing lack of lubrication
motor winding-turns shorted

Pump - wear of the journal bearing

The final verification testing was set up to investigate the vibration envelope detector operation for each type of failure. The failures were induced into the motor in the following manner and tests were run in the following order:

1. Initial Operation. The pump was operated in the same condition as the earlier initial runs to allow comparison of the VED operation with earlier data and to insure repeatability.

2. New Ball Bearings. The two bearings in the motor were replaced with new bearings to obtain a baseline for new, unused bearings and also to compare the new bearing results with earlier data in which the bearings were suspected of slight degradation.

3. Damaged Bearing. A ball was brinelled by impact. This bearing was then installed in the pump end of the motor and operated. Following operation, the location of the damaged bearing was changed to the opposite end of the motor. In each case a new bearing was used along with the damaged bearing.

4. Lack of Lubrication. In order to simulate low lubrication, a new bearing was completely cleaned. The bearing was then dipped in a mixture of oil and solvent. The solvent was then allowed to evaporate leaving only a partial oil film in the bearing. The bearing was then operated in the pump end of the motor.

5. Shorted Motor Turns. It was found that the motor would not turn the pump unit with one winding open. Magnetic field unbalance was, therefore, simulated by inserting a 4.7 ohm resistance in series with one phase of the motor. The pump would operate in this condition, however, speed was greatly reduced.

6. Pump Shaft/Journal Rub. It was concluded that the easiest way

to simulate the real condition would be to operate the pump without water. In order for a realistic situation and one which would not immediately damage the pump, the water would be drained but no attempt would be made to remove the water from the journal. This area would slowly dry out and start to rub. The pump was operated in this condition.

7. Secondary Failure. As will be described, the journal suffered sufficient wear in test 6 to allow the impeller to impact the end of the journal housing. The pump was then operated with water to analyze this type of failure.

Use of the Vibration Envelope Detector

Data from initial runs were analyzed either by use of the real time analyzer following the envelope detection or by the oscilloscope for peak amplitudes. It is important in comparing the readings of the VED to earlier spectral data to understand the relationship between signal-to noise ratios S/N and filter band widths. The real time analyzer was used to plot data from zero to 1,000 Hz. For this frequency span, the equivalent filter band width is two Hertz. The VED uses a tunable band pass filter which is switched-in following the envelope detector. The filter band width is a constant percentage of the center frequency. The percentage chosen is 10 percent. The band width versus frequency is plotted as the dashed curve in Figure 26. The ability of a filter to separate a discrete signal from the noise background is a function of the band width of the filter. A measure of this ability is the resulting signal-to-noise amplitude obtained when using the filter. This is measured by the ratio of the amplitude when the filter is centered at the signal of interest to the amplitude when it is detuned so as not to include the signal; this assumes random noise background. In spectral plots (for example, Figure 5), the signal-to-noise ratio is the ratio of the amplitude of the peak to the noise background. The signal-to-noise ratio for a filter varies inversely with the square root of the filter band width.

Since the 10 percent filter chosen is equal in bandwidth to the real time analyzer only at its low-frequency point of 20 Hz (2 Hz filter bandwidth), at every other point it will be less sensitive to the defect signals than the real time analyzer. The solid curve in Figure 26 is the reduced sensitivity of the VED filter compared to the real time analyzer expressed as a percentage and as a function of frequency.

Reduced sensitivity as used here is a function of the signal to noise ratio (S/N). S/N is important since it relates to the detectability of a signal as the filter is tuned across the band. If a 2 Hz filter were used, the VED needle would respond exactly as the real time analyzer trace, i.e., it would increase by a factor of approximately 12 for the defect signal illustrated in Figure 5. Using the 10 percent

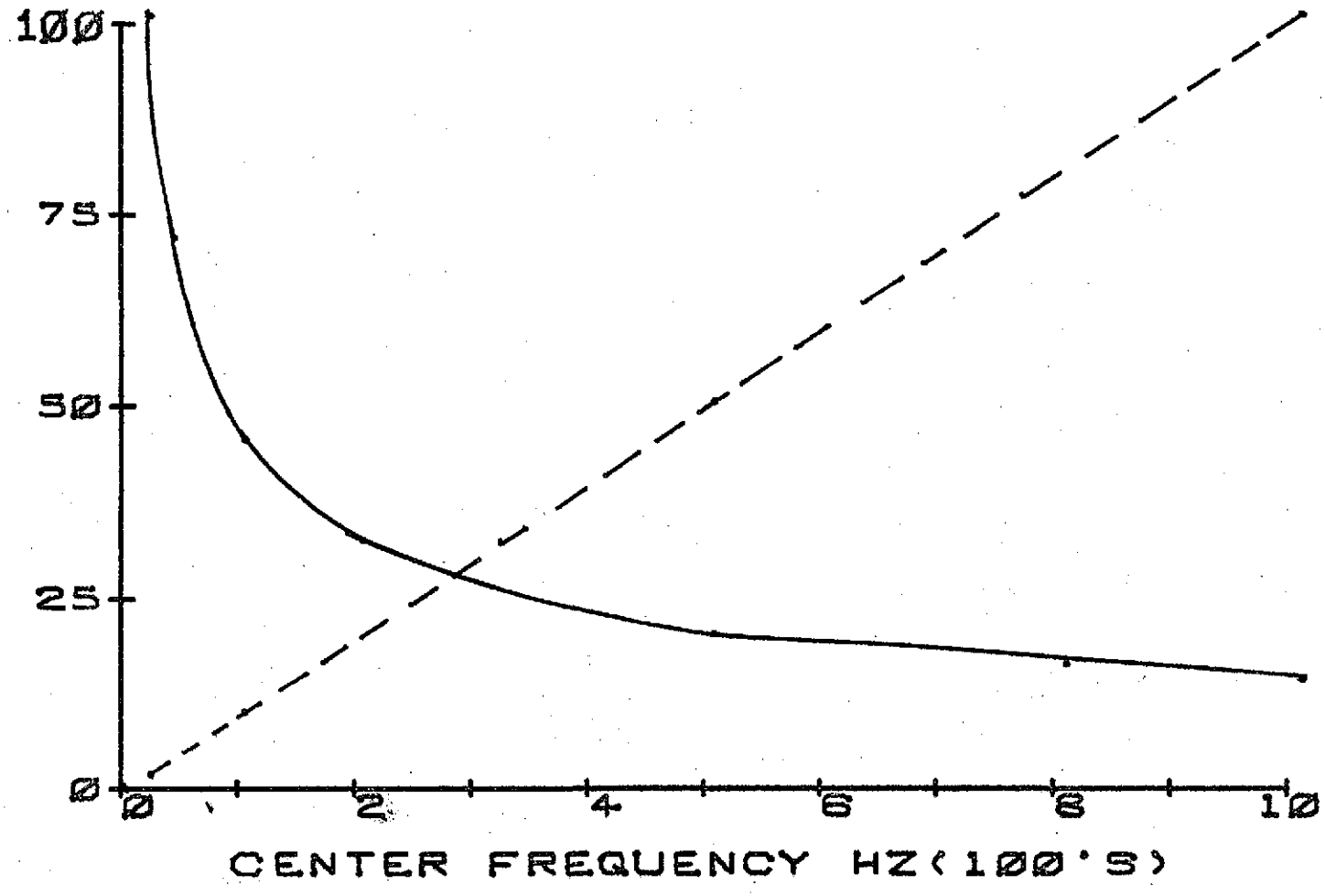

Vertical Axis - Dashed Curve - Filter Band Width - Hz

- Solid Curve - VED Sensitivity Degradation VS. Real Time Analyzer

FIGURE 26 FILTER BANDWIDTH AND SENSITIVITY DEGRADATION VS. FILTER CENTER FREQUENCY

filter in the VED, the same signal at approximately 600 Hz would appear 2.4 times higher than the noise since the sensitivity is degraded to 20 percent as shown in Figure 26. If the S/N ratio is reduced below 1.5, it is assumed that the presence of a discrete signal would not be detected.

All earlier data that was analyzed initially by the real time analyzer was again analyzed using the VED. The results obtained were the same as would have been predicted using the curve of Figure 26 and early spectra. Only the 400 Hz signal of the demodulated 28 KHz resonance would have been detected using the VED. The bearing defect signals and once per revolution shaft rub signals would not have been detected.

The original bearings were disassembled and carefully inspected. No defects were detected. Likewise, the pump journal showed no signs of excessive rubbing. This implies that the added sensitivity of the real time analyzer is not required and in fact can lead to erroneous conclusions. The object of the verification testing is to verify this conclusion.

Two inputs to the VED are available, one accelerometer input and one for voltage sources such as the tape recorder. In using the accelerometer input, the charge sensitivity is used to normalize all accelerometer outputs to 1 mv/g. Details of this procedure are covered in the VED handbook. All data was converted back to this sensitivity so that all numerical data reported is the same that would have been obtained using the VED alone with the accelerometer input.

Verification Test Results

The following discussion of the results obtained during the verification testing assumes that the Vibration Envelope Detector (VED) was used alone to make the decision. Spectra of the demodulated data are included in the appendix that show the results of using a real time analyzer instead of the meter reading of the VED. There were no cases where the defect induced was detectable by the more complicated and expensive use of the real time analyzer and could not be detected by the VED.

Two criteria can be used in the detection of defects. These are:

1. The amplitude of the resonance of interest (28 KHz motor and 35 KHz pump).

2. The amplitude of the known defect signal, as detected by tuning the low-frequency band pass filter to the defect frequency. The S/N must be greater than 1.5.

TABLE IV

RESONANCE AMPLITUDE VS. DEFECT

Defect or Condition	28KHz Resonance (Motor)	35 KHz Resonance (Pump)
Original Run SRC Unit	80	70
Original Run NAS Unit	160	95
Good Bearing	180	--
Defective Bearing Accelerometer and Bearing Outboard End	1100	--
Defective Bearing Accelerometer and Bearing Pump End	1050	
Defective Bearing Bearing Outboard, Accelerometer Pump End	402	
Lightly Lubricated Bearing	180	
Phase Unbalance	180	
Pump Journal Rub		*
Pump After Damage		480

* Tape recorder overdriven

TABLE V

VED READING AND S/N VS. DEFECT

Defect or Condition	Defect Frequency	VED Reading	S/N
Defective Bearing Bearing Pump End Accelerometer Pump End	600 Hz	3000	3.3
Defective Bearing Bearing Outboard End Accelerometer Outboard End	600 Hz	2500	2.1
Defective Bearing Bearing Outboard End Accelerometer Pump End	600 Hz	700	1.75
Unbalanced Phase	200 + 400 Hz	96	1.71
Dry Pump Start	190 Hz	*	1
Dry Pump Finish		*	2.5

* Tape Recorder Overdriven

Table 4 lists the resonance amplitude versus the defect for all the defects induced in the verification tests. Table 5 shows the defect frequency, the signal amplitude, and the signal-to-noise ratio for each of the defects induced. In each case the data are given for the original tests on the pump and the case for the new bearings installed along with the proper inverter voltage used.

All readings are what would be obtained if the VED were set at maximum gain. This condition would use the gain of ten in the charge amplifier and a gain of 200 in the voltage amplifier. When the low-frequency band pass filter is used, it has a gain of 10. Full-scale reading on the meter is taken as 1,000. As can be seen, some readings are greater than full scale. In these cases, less gain would be used to get an actual reading on the meter although for comparison sake the full gain figure is tabulated.

Table 6 summarizes the results. Four columns are shown as follows:

Column	Detection
A	Defect detected by both increase in resonance amplitude and S/N ratio of 1.5 or greater for defect signals.
B	Defect detected by an increase in resonance amplitude but not by an increase in S/N of defect signal.
C	Defect detected by an increase in the S/N ratio of the defect signal but not accompanied by a significant increase in the resonance.
D	Defect not detected by either condition.

The characteristics of each defect detection are discussed below. Condition 2, new ball bearings, is discussed first.

Cond. 2. New ball bearings were installed and a 28 V D.C. was used on the inverter. In this condition, the resonance at both 28 KHz and 35 KHz were low and no discretes were detected in the demodulation signals. This is considered the base line case.

Cond. 1. Initial operation. The NAS (final test unit) unit, as originally operated, had a higher motor resonance at 28 KHz; however, both pumps were in excellent condition so that the difference is considered the normal spread. The demodulated data from both

motors showed 400 and 800 Hz signals. These signals have about the same S/N ratio as the 400 Hz signals from the verification tests when the phase was unbalanced by inserting a 4.7 ohm resistor in one lead. In the initial tests the inverter was powered from 24V D.C. It is concluded that operation at this low voltage results in a phase unbalance in the motor as detected by the VED. No other defects were detectable on the initial operation using the VED.

Cond. 3. Damage bearing. Three cases were run. The damaged bearing was operated in either end of the motor with the accelerometer located over the defective bearing and one case where the accelerometer was located at the opposite end of the motor from the defective bearing. All three cases were easily detected both by an increase in the resonance amplitude and the amplitude of the ball rotational defect signal.

4. Lack of lubrication. This defect was not detected. In all probability, the bearing, even with the limited amount of oil, was operating on an adequate film to prevent damage.

5. Shorted motor turns. This defect, simulated by the insertion of a 4.7 ohm resistor in one phase was detected by an increase in amplitude and S/N ratio of the 200 and 400 Hz signals. The 28 KHz resonance did not increase in amplitude. It is concluded that the proposed test for shorted turns is a valid test and should be employed. It is also noted that a defective bearing will obscure the defective winding signal. It is, therefore, recommended that if defective bearings are detected and replaced, particular attention be paid to the 200 and 400 Hz signals on retest.

6. Pump/shaft journal rub. During the operation of the pump as the journal dried out, the tape recorder gain was inadvertantly increased and some signal clipping resulted. The amplitudes of the signals are, therefore, not valid. The data was analyzed for the presence of the once- and twice-per-rev signals in the demodulated 35 KHz resonance. At the start of the test, these signals were not detectable with the VED (or with the real time analyzer). As the test proceeded, the S/N ratio of the once-per-rev signal increased to 2.5/1 prior to damage to the pump. It is concluded that the use of these signals is a valid diagnostic test for the conditions of pump journal rub.

7. Secondary failure. During the journal rub test, the impeller impacted the end of the journal housing and the test was terminated. The pump was then operated in a normal manner on water with the proper tape recorder gains. The amplitude of the 35 KHz resonance increased greatly and had a low repetition rate indicating impacts were still occurring in the pump.

TABLE VI

SUMMARY OF DETECTION RESULTS

Defect	A	B	C	D
Defective Bearing any Location	X			
Light Lube Bearing				X
Phase Unbalance			X	
Pump Journal Rub		(1)	X	
Pump Impeller Impact		X		

(1) Tape Recorder Overdriven - Data Unreliable

CONCLUSIONS AND RECOMMENDATIONS

Conclusions

The following conclusions were drawn based on the program results:

1. The concept employing the detection of pump defects by the amplitude and modulation characteristics of high-frequency mechanical resonances is a valid concept.

2. The high-frequency resonance technique may be used on radically different pumps such as the gear and centrifugal pump even when the normal vibration levels are an order of magnitude different.

3. The extreme sensitivity that results from analyzing the demodulated spectra produced by a real time analyzer is not required for final defect detection and, in fact, would introduce confusion since defect signals would be detected prior to real damage to the pump.

4. The real time analyzer can be used in conjunction with the VED for initial pump testing to predict VED levels and frequencies of interest for defects.

The Vibration Envelope Detector is an easy-to-use device. As modified in the final testing to give the low-frequency band pass filter a gain of 10, the sensitivity and filter band widths appear to be optimum for defect detection.

Recommendations

The following recommendations are made for further implementation of the Vibration Envelope Detector delivered to NASA and for further investigation of the diagnostic technique:

1. The Vibration Envelope Detector should be used in conjunction with pump testing at NASA-MSFC. In each application the following steps should be taken:

    a. Analyze the pump for the failure modes possible and probable.

    b. Calculate the impact or rub repetition rates associated with the probable failure modes.

c. During initial testing, data should be recorded on magnetic tape from several different accelerometer locations. Tape recorder frequency response should be to 100 KHz.

d. Laboratory instrumentation should be used to supplement the Vibration Envelope Detector on initial tests, particularly if the pump is operating normally. The real time analyzer, as used during this program, will allow selection of the proper resonance to monitor with the vibration envelope detector from the data generated by normally-operating pumps.

e. Based on the results of the initial data analysis, derive a set of detection criteria for the failure modes predicted.

f. Employ these detection criteria and the Vibration Envelope Detector on continued pump testing. Verify the defect detection criteria by pump teardown and inspection when the Vibration Envelope Detector indicates that a component condition is deteriorating.

g. Based on the results of the pump testing, develop a set of final detection criteria to be used to inspect shuttle booster pumps between flights.

2. Inadequate lubrication in a lightly-loaded ball bearing is probably the primary cause for failure of these components. Simulation of this type of failure is extremely difficult and the single test during this program was not successful. In order to determine if the high-frequency vibration technique can be used to detect a dangerously low lubricant level, a carefully controlled laboratory test should be conducted. In this test the vibration character should be correlated with lubricant film thickness measurements to determine when metal to metal contact occurs. Electrical resistance measurements across the bearing have been successfully used for this purpose.

REFERENCES

1. Broderick, J. J., Burchill, R. F., and Clark, H. L., "Design and Fabrication of Prototype System for Early Warning of Impending Bearing Faults", Prepared under Contract NAS8-25706 for NASA-MSFC by MTI, Latham, N.Y.

2. Burchill, R. F., "Resonant Structure Techniques for Bearing Fault Analysis". Paper Presented at 18th Meeting of the Mechanical Failures Prevention Group, Gaithersburg, MD., November, 1972.

3. Burchill, R. F., Frarey, J. L., and Wilson, D. S., "New Machinery Health Diagnostic Technique Using High Frequency Vibration". Paper 730930 Presented at the SAE National Aerospace Engineering and Manufacturing Meeting, Los Angeles, CA. October, 1973.

4. Balderston, H. W., "The Detection of Incipient Failure in Bearings". Presented at the 28th National Fall Conference of the American Society for Nondestructive Testing, Detroit, MI. October, 1968.

5. James, Reber, Baird, and Neale, "Application of High Frequency Acoustic Techniques for Predictive Maintenance in a Petrochemical Plant." Presented at the 28th Annual Petroleum Mechanical Engineering Conference, Los Angeles, CA. September, 1973.

6. Howard, P., "Shock Pulse Instrumentation" Presented at the 14th Meeting of the Mechanical Failure Prevention Group, Los Angeles, CA. June, 1971.

7. Houser, D. R. and Drosjack, M. J., "Vibration Signal Analysis Techniques." UAS AMRDL Technical Report 73-101, December, 1973.

APPENDIX A

GEAR PUMP INITIAL TESTS
SUPPORTING SPECTRA

Selected Spectra are presented that relate to Table 1 of the report. The conditions included

Figure	Condition
A1	New Pump on Water at 75 psi
A2	Gear tips relieved 0.001" operating at 75 psi
A3	Gear tips relieved 0.002" pump improperly assembled operating at 75 psi
A4	Bushing Bored 0.002" operating at 75 psi
A5	Bushing and idler bored 0.002" operating at 0 psi

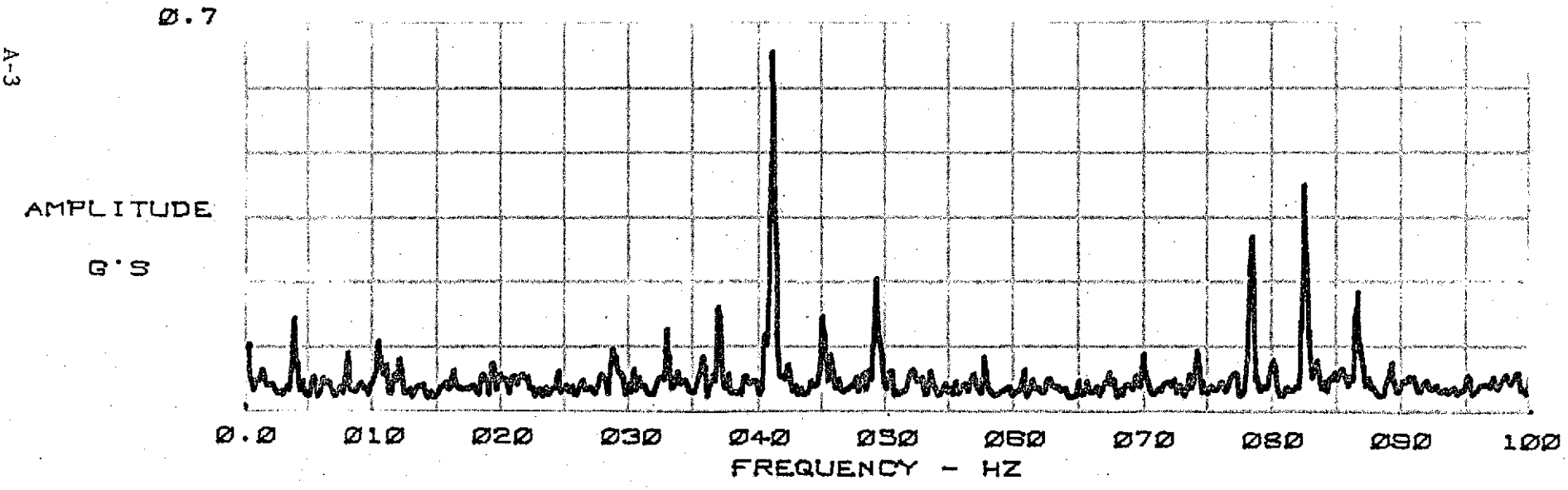

A1 NEW PUMP ON WATER AT 75PSI

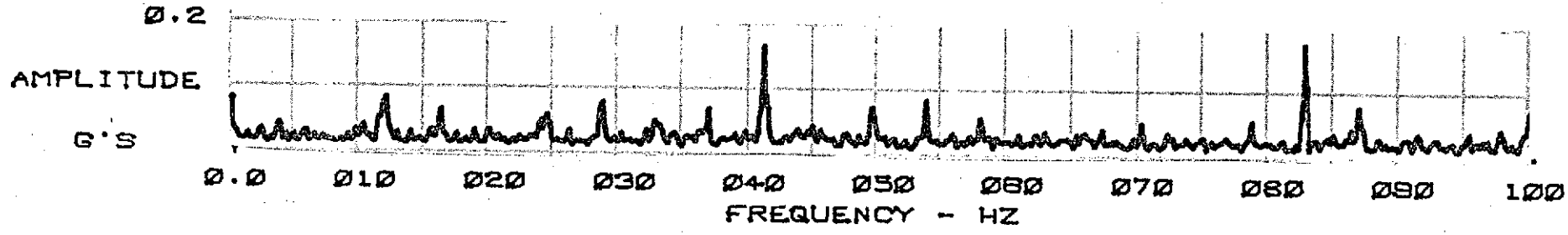

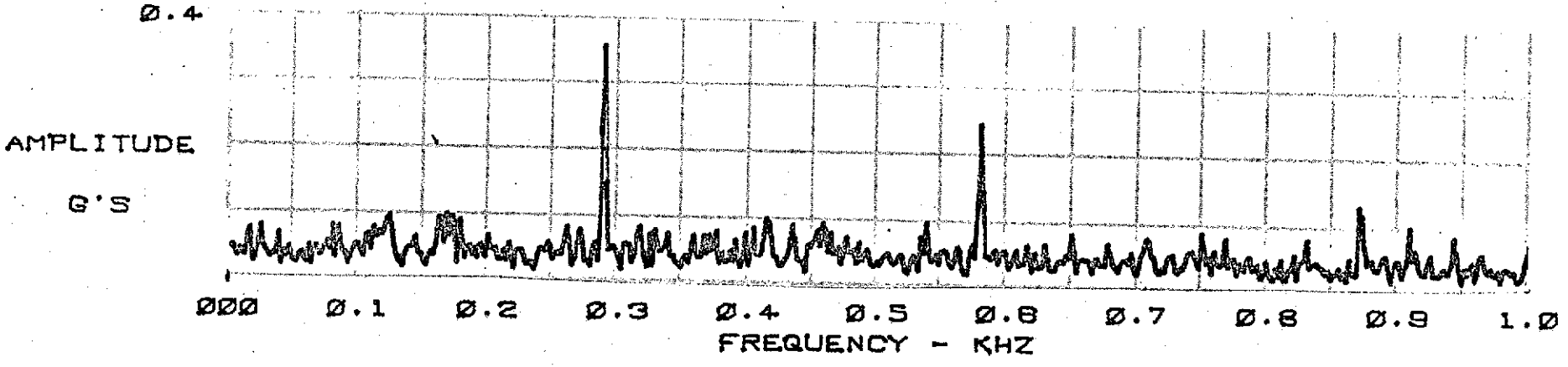

A2 GEAR TIPS RELIEVED Ø.ØØ1-OPERATING AT 75 PSI

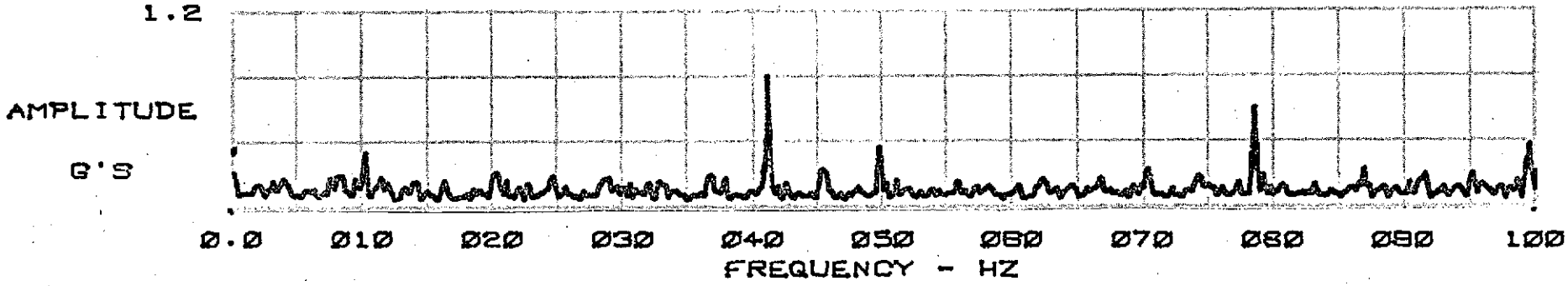

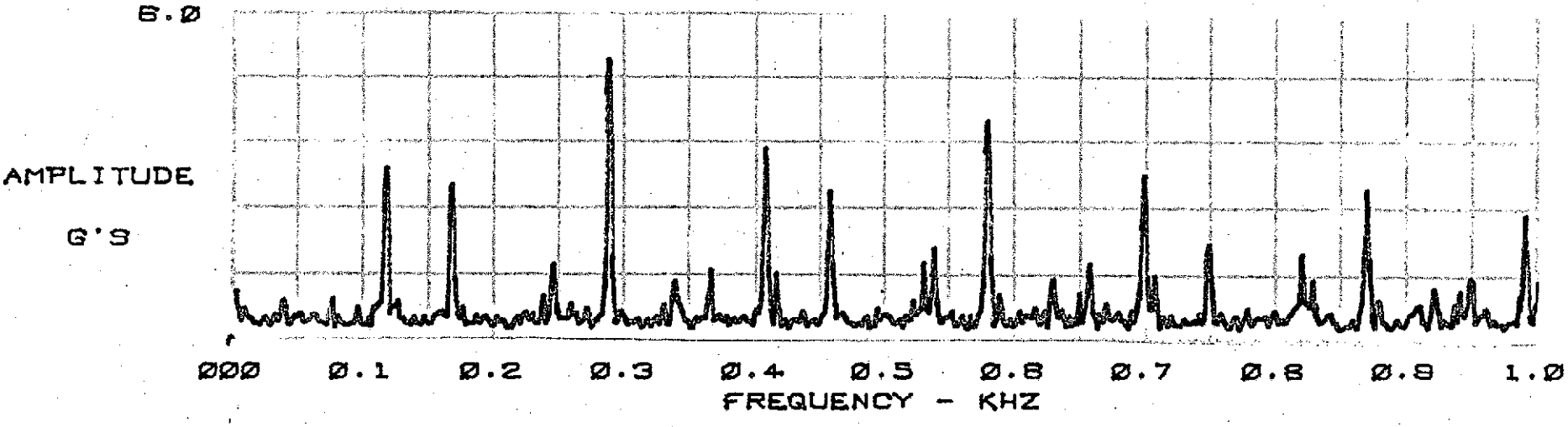

A3 PUMP IMPROPERY ASSEMBLED-OPERATING AT 75 PSI

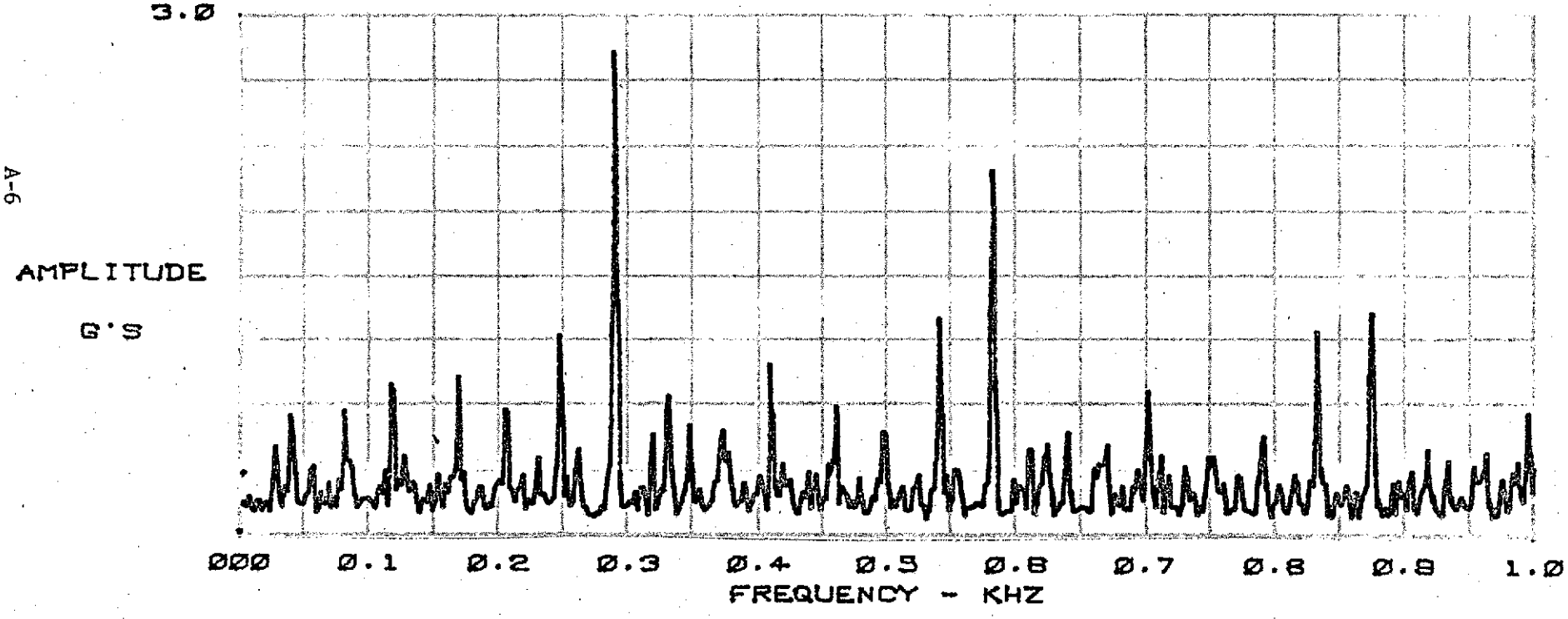

A4A BUSHING BORED Ø.ØØ2-OPERATING AT 75PSI

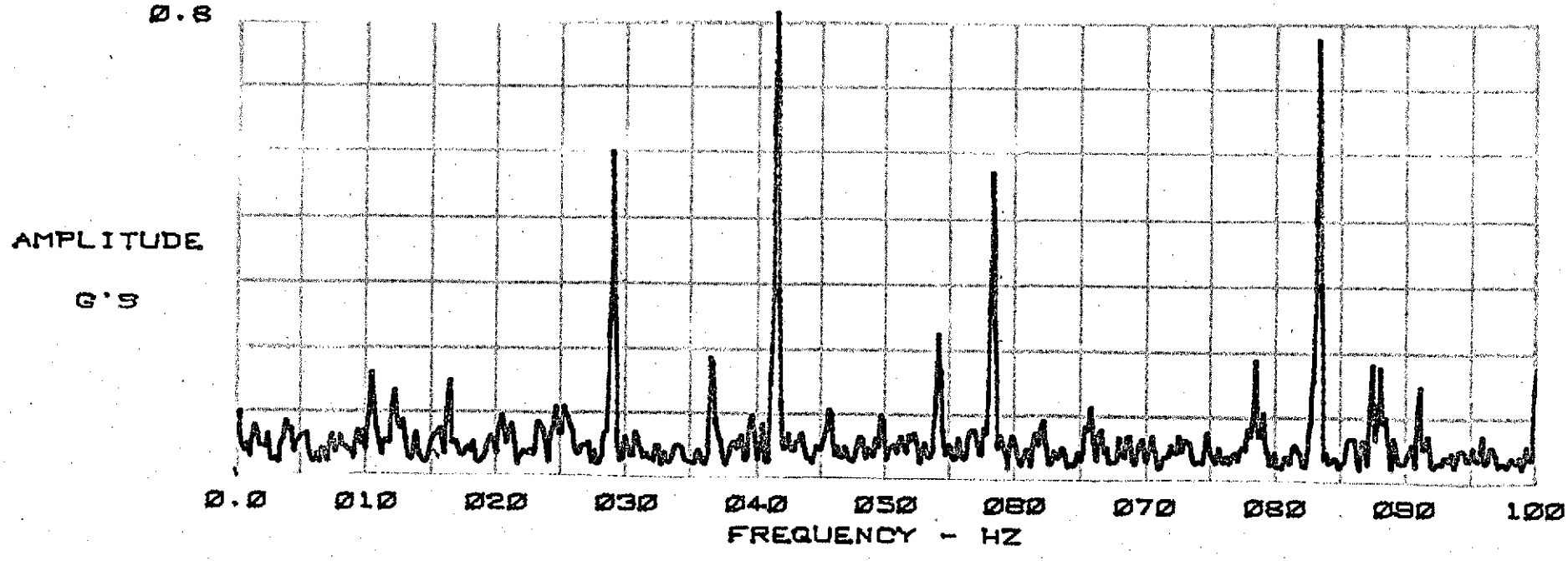

A4-B BUSHING BORED Ø.ØØ2-OPERATING AT 75PSI

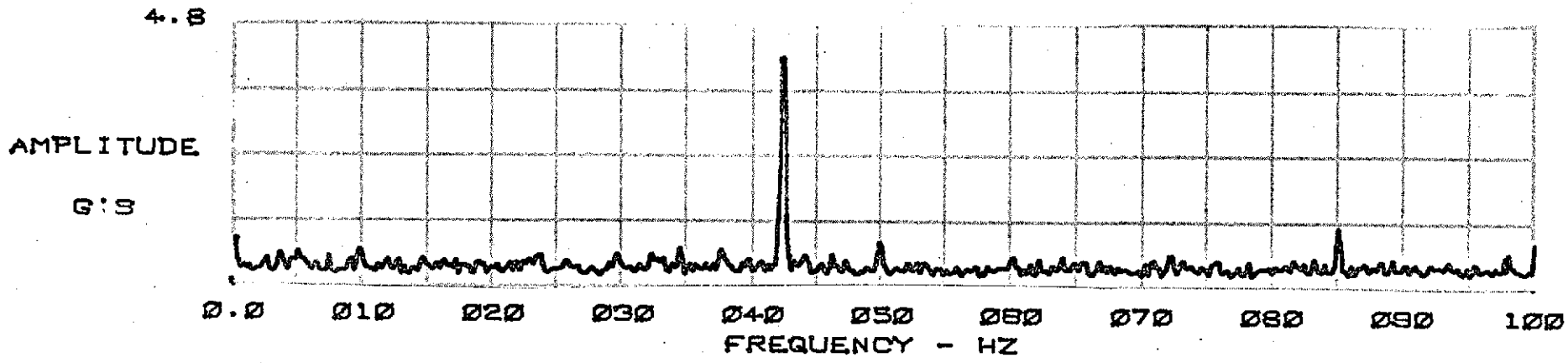

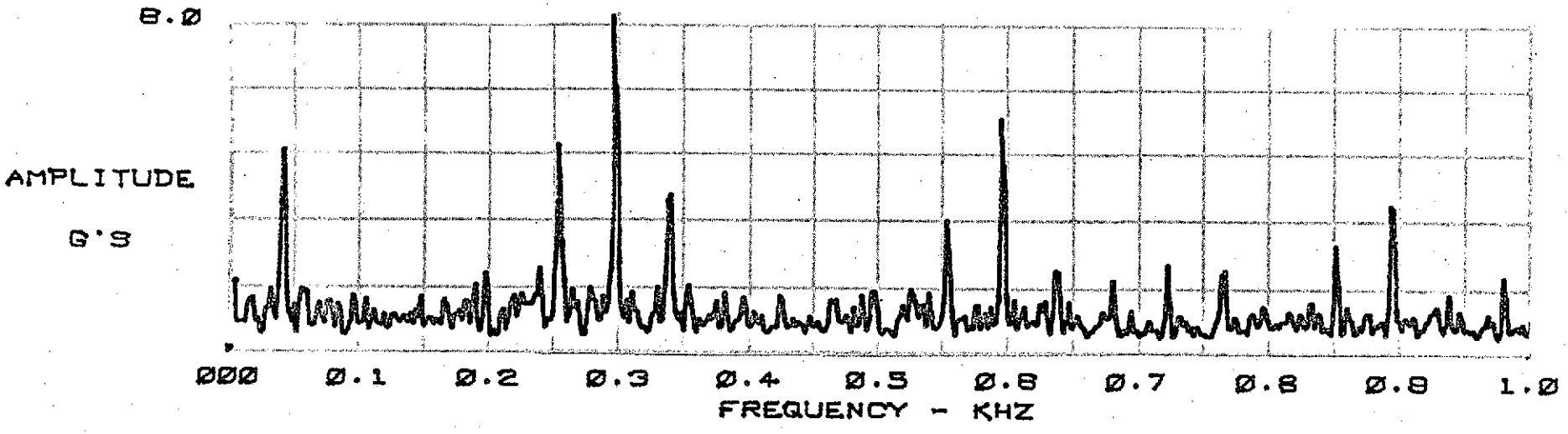

AS BUSHING AND IDLER BORED Ø.ØØ2- AT ØPSI

APPENDIX B

CENTRIFUGAL PUMP INITIAL TEST SPECTRA

Table III in the report gives g values for defect signals identified in the demodulated data. Figures B1, B2 and B3 are a complete set of backup spectra for Table III for the 28 KHz resonance as measured on the SRC unit (the unit Shaker Research Corporation disassembled). Figure B4 is the demodulated 35 KHz spectrum for the SRC unit at 1.5 gpm. Figure B5 is the demodulated 28 KHz spectrum for the NAS unit at 1.5 gpm and Figure B6 is the demodulated 35 KHz spectrum for the NAS unit at 1.5 gpm. The spectra at 1.5 gpm were chosen since this flow range is just below the rated flow of 900 lb/hr.

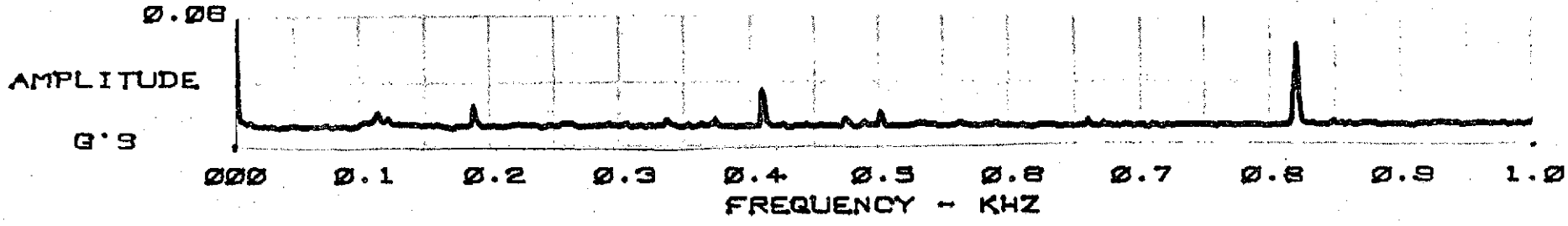

Ø.5 GPM

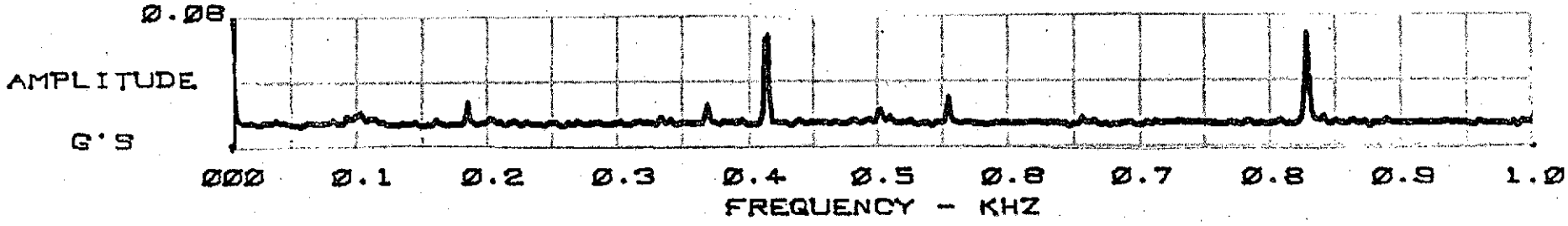

B1 DEMODULATED 28 KHZ SPECTRA SRC UNIT ØGPM

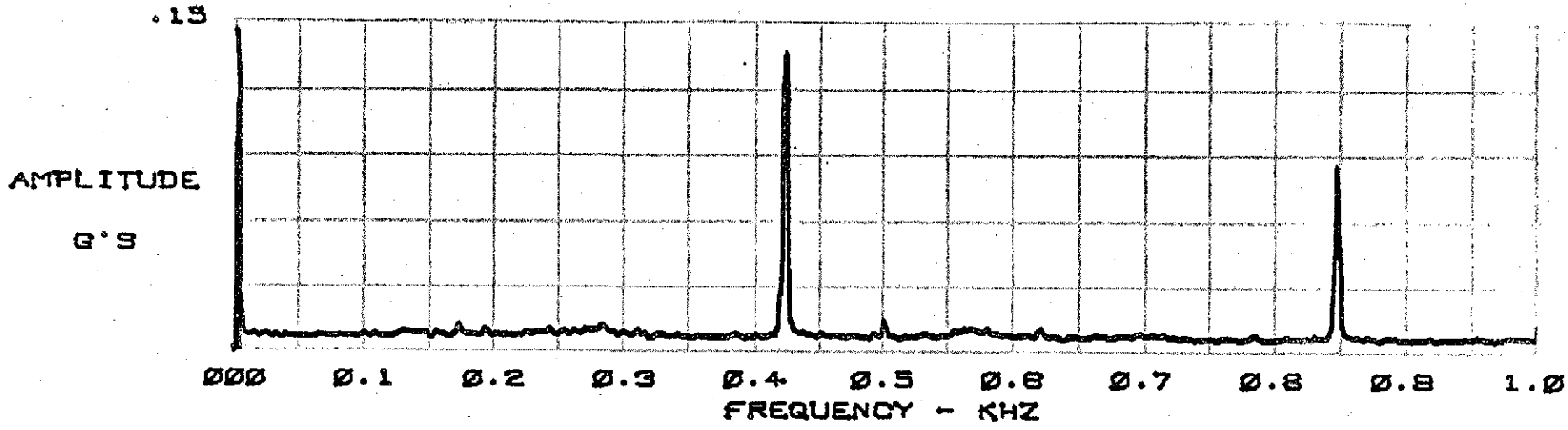

1.5 GPM

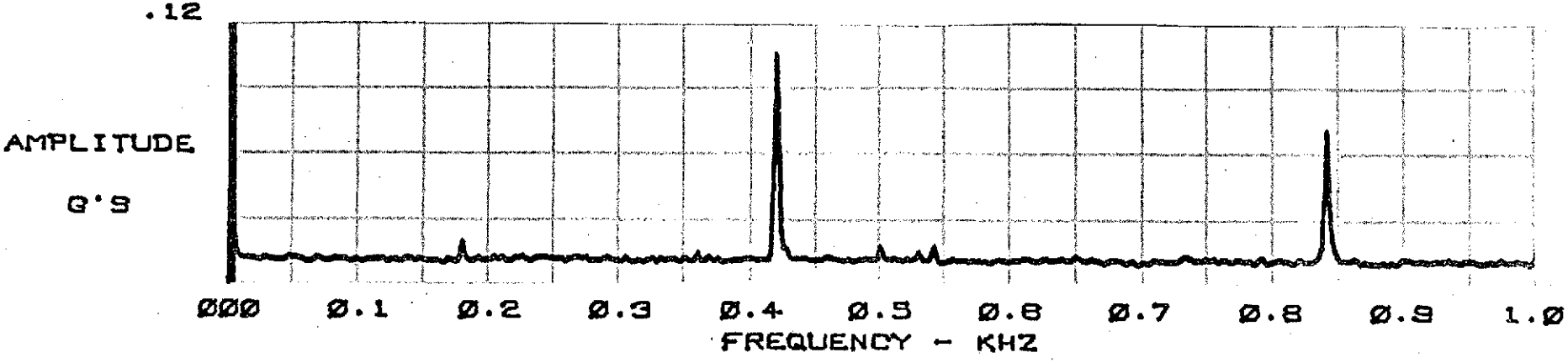

B2 DEMODULATED 28 KHZ SPECTRA SRC UNIT 1.ØGPM

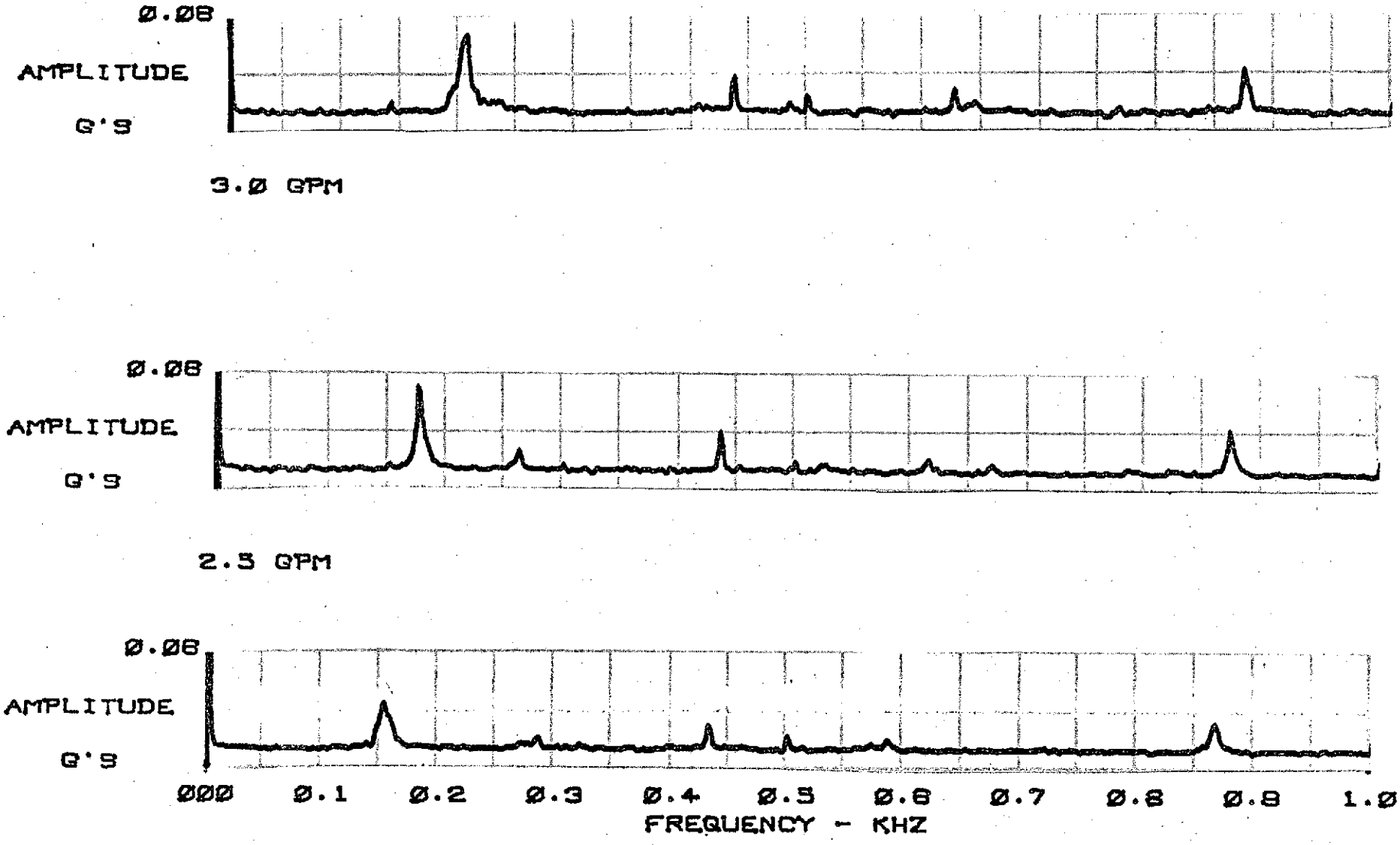

B3 DEMODULATED 28 KHZ SPECTRA SRC UNIT 2.Ø GPM

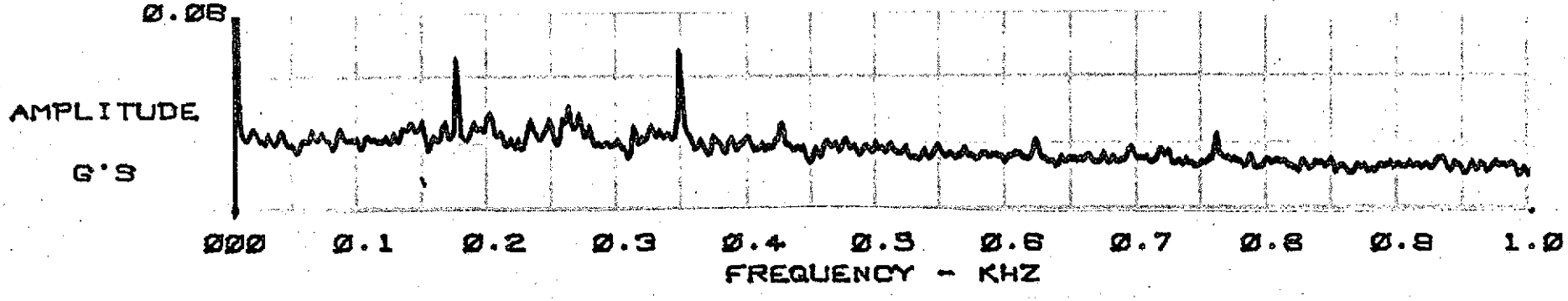

B4 DEMODULATED 35 KHZ SPECTRA SRC UNIT 1.5 GPM

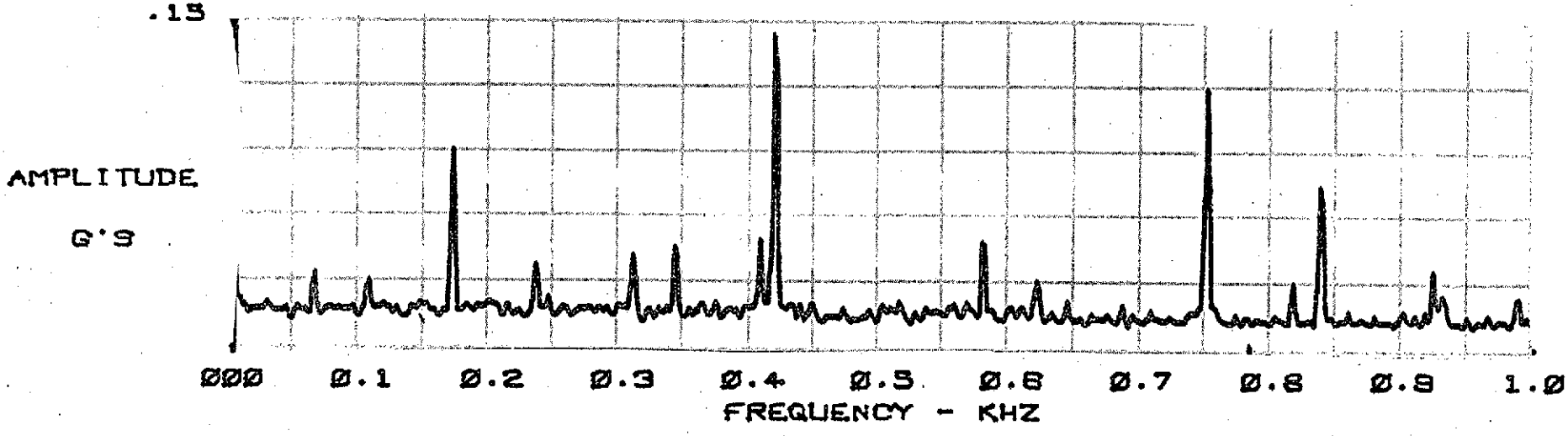

B5 DEMODULATED 28 KHZ SPECTRA NAS UNIT 1.5 GPM

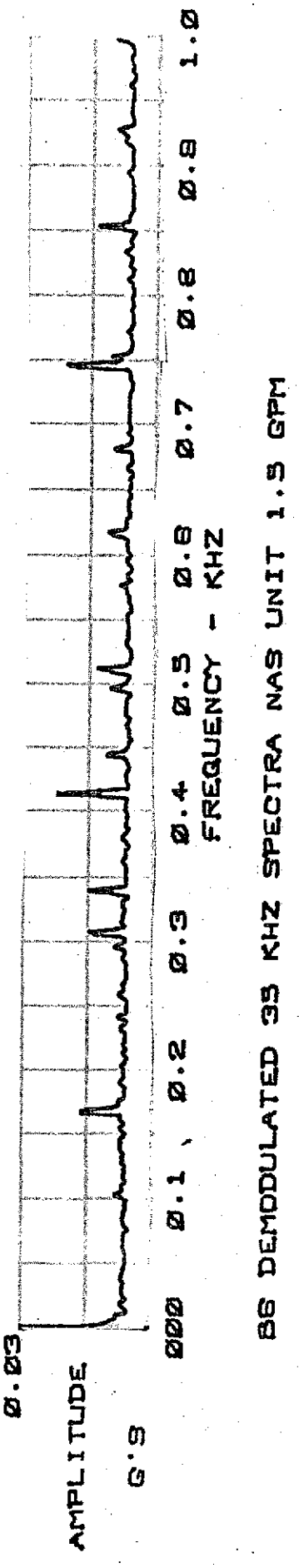

BB DEMODULATED 33 KHZ SPECTRA NAS UNIT 1.5 GPM

ORIGINAL PAGE IS
OF POOR QUALITY